

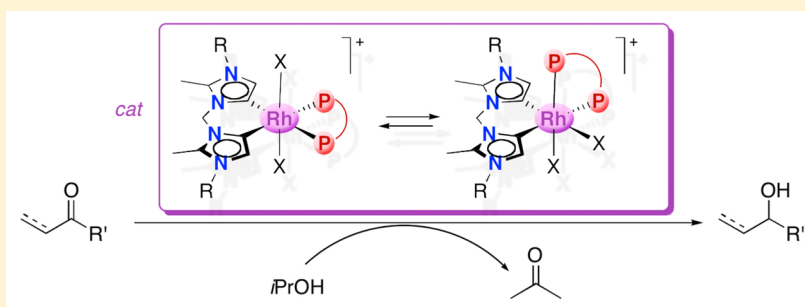
Synthesis, Isomerization, and Catalytic Transfer Hydrogenation Activity of Rhodium(III) Complexes Containing Both Chelating Dicarbenes and Diphosphine Ligands

Kevin Farrell,[†] Helge Müller-Bunz,[†] and Martin Albrecht^{*,†,‡}

[†]School of Chemistry & Chemical Biology, University College Dublin, Belfield, Dublin 4, Ireland

[‡]Departement für Chemie und Biochemie, University of Bern, Freiestrasse 3, 3012 Bern, Switzerland

S Supporting Information



ABSTRACT: Different rhodium(III) complexes $[\text{Rh}(\text{C},\text{C})(\text{P},\text{P})\text{X}_2]^+$ bearing both a *cis*-chelating dicarbene and a diphosphine ligand were synthesized (C,C = methylene(4,4'-diimidazolylidene); P,P = 1,2-bis(diphenylphosphino)ethane (dppe), (*R*)-(+)-2,2'-bis(diphenylphosphino)-1,1'-binaphthalene (*R*-BINAP); X = halide, carbanion, NCMe). Solution analysis by NMR spectroscopy indicate a dynamic behavior of the complexes and *cis/trans* isomerization processes, likely through dissociation of the nonchelating ligands X (X = halide, NCMe), and eventually also involving the diphosphine ligand, identified by the formation of phosphine oxides. The presence of a diphosphine ligand in addition to the dicarbene substantially enhances the catalytic activity of the rhodium center in the transfer hydrogenation of ketones in *i*PrOH/KOH, reaching over 4000 turnover numbers and turnover frequencies around 1000 h^{-1} vs 330 h^{-1} for the phosphine-free analogue. Optimization of the catalytic conditions allowed transfer hydrogenation to be run with only 1 mol % base instead of the often used 10 mol %. The chiral *R*-BINAP ligand enhances catalytic activity, though no enantioselectivity was induced in the transfer hydrogenation of fluoracetophenone as prochiral substrate.

INTRODUCTION

N-heterocyclic carbenes (NHCs) and phosphines are ubiquitous ligands in transition metal catalysis and promote a broad array of catalytic transformations including hydrogenations,¹ C–H activations,² olefin metathesis³ and cross coupling reactions.⁴ In recent years, NHCs have emerged as robust and powerful ligands for stabilizing high oxidation state metal centers due to their generally stronger donor properties than phosphine ligands.⁵ NHCs have been incorporated into many traditionally phosphine-ligated catalysts, sometimes leading to enhanced activity.⁶ While at early stages, this strategy has prompted the view of NHCs as “superphosphine” ligands,⁷ a direct comparison between NHCs and phosphines is obviously prevented by their vastly different steric effects and diverging bonding properties.⁸

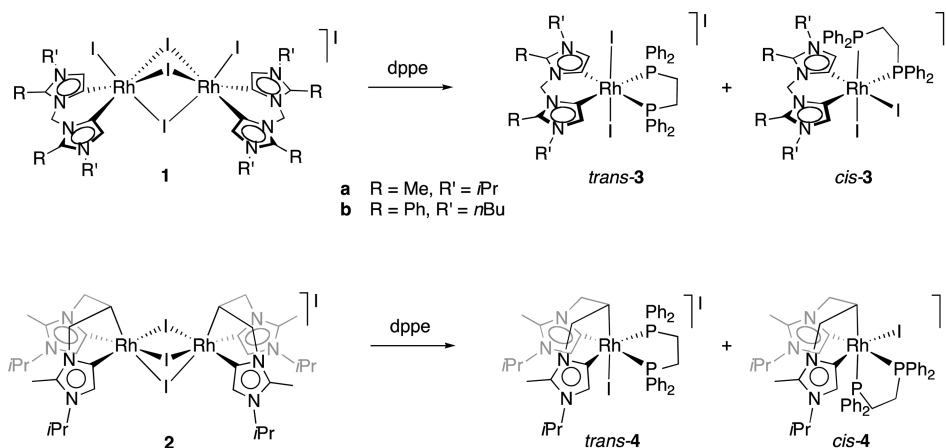
Even though replacement of phosphine ligands with NHCs has been highly prolific and well-investigated, much less work has been directed toward complexes containing NHCs and phosphines as complementary ligands at the same metal center.⁹ This underdevelopment is particularly remarkable

when considering the development of Grubbs' second generation olefin metathesis catalyst,³ which was undoubtedly one of the hallmark achievements¹⁰ that spurred the application of NHCs as spectator ligands in transition metal catalysis.^{3–5} In these olefin metathesis catalysts, incorporation of a NHC ligand only led to an improved catalytic activity with a mixed phosphine/NHC ligand pattern,¹¹ while the bis(NHC) complex was much less active.¹² The lability of the phosphine ligand and the more covalent $\text{C}_{\text{NHC}}\text{--Ru}$ bond work complementary to each other to enhance the activity of the catalyst.¹³ Similar enhancement of catalytic performance has been observed in palladium complexes that were used for olefin and alkyne hydrogenation, and alcohol dehydrogenation.¹⁴ Here we report our work on applying this concept on rhodium(III) systems by installing both phosphine ligands and abnormal carbene ligands.¹⁵ Abnormal carbenes exhibit exceptionally strong donor characteristics for formally neutral

Received: September 22, 2015

Published: December 16, 2015

Scheme 1. Synthesis of Dicarbene dppe Rhodium(III) Complexes 3 and 4



ligands, and impart in many cases advantageous catalytic properties.¹⁶ The utilization of chelating dicarbene and diphosphine ligands provides substantial benefits for the rhodium center to catalyze transfer hydrogenation reactions.

RESULTS AND DISCUSSION

Synthesis of Dicarbene dppe Rhodium(III) Complexes. The known¹⁷ dimeric rhodium(III) complexes **1** and **2** were suitable precursors for phosphine coordination, each of these complexes containing a C4-bound diimidazolylidene chelate (Scheme 1). Reaction of complexes **1** and **2** with 1,2-bis(diphenylphosphino)ethane (dppe) afforded the monometallic complexes **3** and **4**, respectively. Cleavage of the dimeric structure was indicated by the well-resolved ¹H NMR signals in CD₂Cl₂. The single set of imidazolylidene resonances for *trans*-**3a** suggests two magnetically equivalent, symmetry-related carbene ligands. The methylene group linking the two heterocycles appears as a sharp singlet ($\delta_{\text{H}} = 7.2$), pointing to a fast inversion of the boat-like six-membered metallacycle. In the ¹³C NMR spectrum, the carbenic carbon of *trans*-**3a** resonates as a doublet of doublets centered at $\delta_{\text{C}} = 134.9$ due to coupling to ¹⁰³Rh and two different ³¹P nuclei ($^1J_{\text{CRh}} = 32.8$ Hz, $^2J_{\text{CP}^{\text{cis}}} = 9.7$ Hz, $^2J_{\text{CP}^{\text{trans}}} = 147$ Hz). This signal pattern combined with the data from ¹H NMR spectroscopy and the presence of a single doublet in the ³¹P NMR spectrum at $\delta_{\text{P}} = 20.3$ ($^1J_{\text{PRh}} = 76.2$ Hz) indicates a C_s-symmetric complex *trans*-**3a** in solution with enantiotopic phosphorus atoms and with the iodide ligands in mutual *trans* position. However, upon standing for extended periods of time, gradual isomerization of *trans*-**3a** was observed in solution. Two emerging doublets of doublets at $\delta_{\text{P}} = 48.3$ ($^1J_{\text{PRh}} = 118.4$ Hz, $^2J_{\text{PP}} = 7.7$ Hz) and 19.6 ($^1J_{\text{PRh}} = 81.6$ Hz) ppm indicated formation of the C₁-symmetric isomer *cis*-**3a** containing the iodide ligands in mutual *cis* position, one *trans* to a carbene, and the other *trans* to a phosphine ligand. The larger Rh–P coupling constant was attributed to the phosphine *trans* to iodide, while the smaller constant is similar to that observed in *trans*-**3a** ($^1J_{\text{PRh}}$ 81.6 Hz vs 76.2 Hz), thus supporting a phosphine *trans* to an abnormal carbene ligand. This isomerization suggests that the all-*cis* isomer is kinetically less preferred, but thermodynamically the most favored configuration, corroborated also by a solid state analysis of *cis*-**3b**.^{17a} Indeed, analogous isomerization of *trans*-**3b** to *cis*-**3b** was observed on standing in solution, with ³¹P NMR chemical shifts and coupling constants almost identical to those of *trans*- and *cis*-**3a**, respectively.¹⁸

The isomerization of *trans*-**3a** to *cis*-**3a** is gradual in CDCl₃ with an initial 6:1 mixture that converts to an approximate 2:3 ratio after 5 days. The isomerization in CD₂Cl₂ is more than 1 order of magnitude slower and after 3 weeks the *cis* and *trans* isomers were present in about equal ratios. This rate dependence suggests that solvent polarity may be relevant, presumably for stabilizing a transient dicationic intermediate generated through reversible I[−] dissociation. In addition to the isomerization, traces of dppe oxide were observed over this time frame, suggesting slow phosphine dissociation from the rhodium coordination sphere when stored in CD₂Cl₂ for prolonged time.¹⁹

The reaction of the C,C,C-tridentate carbene rhodium dimer **2** with dppe gave a more complicated ³¹P NMR spectrum with signals for four different species. Two of these were comprised of magnetically identical phosphines, while the other two gave rise to AB patterns and revealed a dissymmetric dppe ligand. The two major isomers were assigned to C_s-symmetric *trans*-**4** and C₁-symmetric *cis*-**4** (where *trans* and *cis* refer to the relative position of iodide to the carbanion ligand CHR₂[−]; cf. Scheme 1). Both species feature similar Rh–P coupling constants ($^1J_{\text{PRh}} = 83.7$ Hz for *trans*-**4**; $^1J_{\text{PRh}} = 78.3$ and 82.0 Hz for *cis*-**4**). These coupling constants are in the same range as those in the bidentate dicarbene dppe complexes **3**. Accordingly, the *trans* influence of the carbene and the anionic alkyl carbon are similar, underpinning the exceptionally strong donor properties of these mesoionic carbenes and their strong relationship with carbanionic ligands.

The two minor isomers both featured substantially deshielded ³¹P resonances. For example, the higher symmetry species has $\delta_{\text{P}} = 57.4$ vs $\delta_{\text{P}} = 28.9$ in *trans*-**4**. Moreover, the Rh–P coupling constants are markedly increased with $^1J_{\text{PRh}} = 131.3$. The minor unsymmetric species showed one similarly large coupling constant of 137.6 Hz ($\delta_{\text{P}} = 50.0$) and a smaller one 80.0 Hz ($\delta_{\text{P}} = 29.8$ ppm). These larger coupling constant suggest either a change of geometry or a significant electronic change at the rhodium center. Electronic changes might ensue from iodide dissociation and the formation of a dicationic rhodium(III) solvato complex, though solvent coordination seems less probable in weakly coordinating solvents such as those used for NMR spectroscopic analyses (CDCl₃, CD₂Cl₂). Geometrical changes may include the formation of a pentacoordinate system, or a *fac*- to *mer*- change of the tridentate dicarbene ligand, or a combination of these processes.^{17,20} The low fraction of these minor components

and their similar properties to complex **4** prevented a more in-depth analysis.

The ^1H NMR signals for the aromatic heterocyclic protons for *trans*-**4** appear as a low field singlet ($\delta_{\text{H}} = 7.22$), while those of *cis*-**4** are magnetically inequivalent and appear as two singlets at $\delta_{\text{H}} = 6.59$ and 4.36 ppm. The remarkable upfield shift of the latter resonance suggests strong shielding, presumably imposed by a phenyl group of the dppe ligand. While the ^{13}C NMR signals for the carbenic nucleus were not resolved for any isomer of **4**, the rhodium bound alkyl carbon resonance was detected for *cis*-**4** as a doublet of doublet of doublets at $\delta_{\text{C}} = 36.7$ due to coupling with rhodium ($^1J_{\text{CRh}} = 20.9$ Hz) and both phosphorus atoms ($^2J_{\text{CPtrans}} = 93.0$ Hz, $^2J_{\text{CPcis}} = 5.4$ Hz).

Similar to complexes **3a,b**, the isomeric mixture of **4** was also unstable in solution at room temperature over extended periods of time and revealed the slow formation of dppe oxide in CD_2Cl_2 .²¹ The formation of dppe oxide indicates that in both complexes the diphosphine ligand has some lability, perhaps imparted by the strong *trans* effect of the dicarbene ligand. Phosphine dissociation may be fast and reversible, unless the phosphine is oxidized, thus leading eventually to the observed decomposition products. When complexes **3** and **4** were stored as CD_2Cl_2 solutions at 4 °C instead of room temperature, they were completely stable over several months and no dppe oxide or other decomposition products were detected.

A crystal structure determination of *trans*-**4** confirmed the arrangement of the ligands deduced from solution analysis (Figure 1).²² The rhodium center is in a distorted octahedral

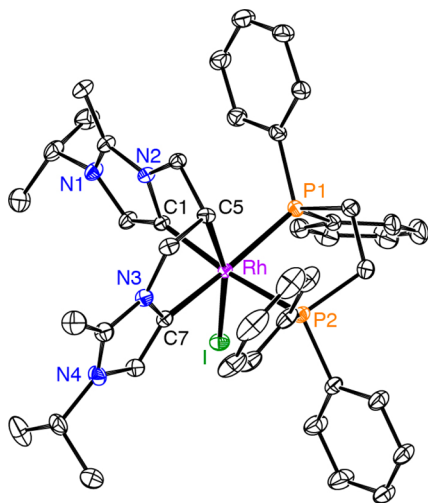


Figure 1. ORTEP representation of *trans*-**4** (50% probability ellipsoids, hydrogen atoms, cocrystallized solvent molecules, and iodide counterion omitted for clarity); selected bond lengths and angles: Rh–C1 2.024(2) Å, Rh–C7 2.025(2) Å, Rh–C5 2.158(2) Å, Rh–P1 2.3401(6) Å, Rh–P2 2.3516(6) Å, Rh–I 2.7490(2) Å, C7–Rh–C1 88.31(8)°, C5–Rh–I 165.24(6)°.

geometry, with *trans*-positioned alkyl and iodide ligands, C5–Rh–I 165.24(6)°. The dicarbene bite angle is 88.3° and thus some 5° larger than in a related complex containing two MeCN ligands instead of the chelating diphosphine,^{17b} suggesting some flexibility in the tridentate bonding. The Rh–C_{NHC} bonds are relatively long, 2.025(2) Å when *trans* to the dppe ligand,²³ which is expected when considering the stronger *trans* influence of phosphine compared to NCMe (Rh–C_{NHC} 1.96 Å in the MeCN analogue). The Rh–C_{alkyl} bond is 2.158(2) Å and thus considerably longer than the Rh–C_{NHC} bonds.

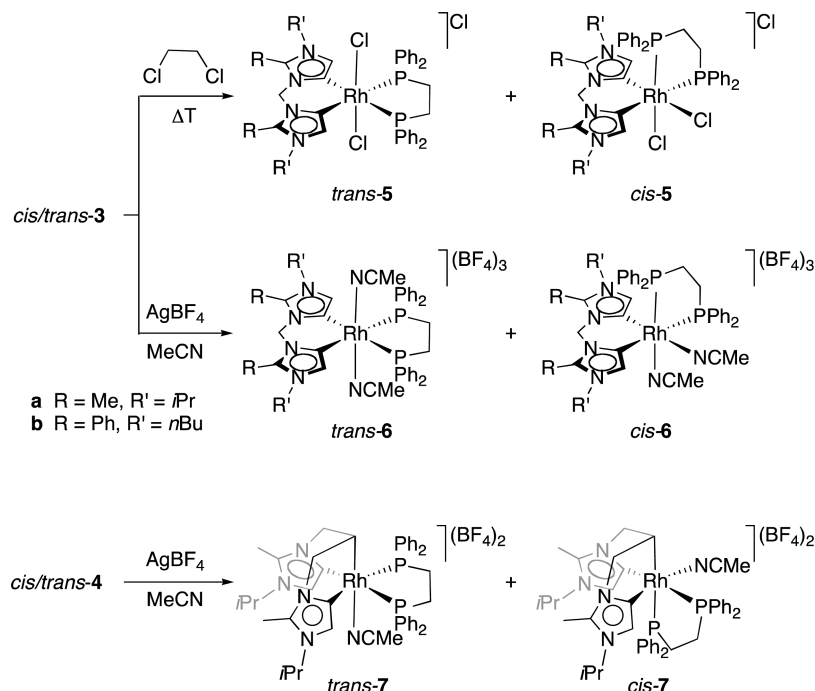
Ligand Exchange Reactions. Reflux of complex **3a** in 1,2-dichloroethane induced halide exchange and installed two chloro ligands at the rhodium center to yield complex **5** quantitatively (Scheme 2). The complete exchange of all three iodides was confirmed by elemental analysis and mass spectrometry, and likely involves a Finkelstein reaction, i.e., substitution of chloride in the solvent by metal-decoordinated iodide.²⁴ NMR spectroscopy indicated the presence of *cis*- and *trans*-**5** in a 3:1 ratio, corroborating the *cis*-isomer to be thermodynamically more stable. The ^{31}P NMR signals of *cis*-**5** were shifted downfield compared to those of *cis*-**3a** and appeared at $\delta_{\text{P}} = 53.9$ ($^1J_{\text{PRh}} = 123.7$ Hz) and 28.7 ($^1J_{\text{PRh}} = 81.6$ Hz; Table 1). The larger Rh–P coupling constant of the low-field resonance is in agreement with a smaller *trans* influence of Cl^- vs I^- .²⁵ In the chloro complex, the carbenic carbon resonances were well resolved. One carbon resonance appeared as a doublet of doublet of doublets due to coupling with rhodium, a *trans* phosphorus and a *cis* phosphorus ($\delta_{\text{C}} = 141.0$ ppm; $^1J_{\text{CRh}} = 33.1$ Hz, $^2J_{\text{CPcis}} = 13.0$ Hz, $^2J_{\text{CPtrans}} = 149.5$ Hz), while the other carbene carbon appeared as a doublet of triplets due to coupling to rhodium and two *cis*-positioned phosphorus atoms ($\delta_{\text{C}} = 135.4$ ppm; $^1J_{\text{CRh}} = 40.3$ Hz, $^2J_{\text{CP}} = 9.0$ Hz).

Complexes **3** and **4** reacted smoothly with AgBF_4 in MeCN and gave the corresponding solvento complexes **6** and **7**, respectively (Scheme 2). The ^{31}P NMR signals shifted significantly downfield upon halide abstraction, e.g., *cis*-**6a** featured two doublets of doublets at $\delta_{\text{P}} = 59.4$ and 44.3 (Table 1). The coupling constants for the tricationic complexes **6** were similar to those of the chloro complexes **5**, and thus in agreement with a similar *trans* influence of Cl^- and MeCN. According to ^{31}P NMR spectroscopy, isomer *trans*-**6** was initially formed as the major isomer, though over 3 h, the mixture equilibrated at 1:1 *cis/trans* ratio for both complexes **6a** and **6b**. This isomerization is faster than in complex **3**, supporting the fact that dissociation of the monodentate ligand is indeed critical for the *trans*–*cis* isomerization.

The reaction of complex **4** with AgBF_4 gave four species. The two major components showed the same chemical shift and coupling constants as the ^{31}P NMR spectrum of **4** in CD_3CN , suggesting facile iodo for MeCN exchange in this complex. The two minor species were more deshielded and showed large Rh–P coupling constants (>130 Hz). The formation of four new species upon halide abstraction suggests that the unidentified minor isomers of **4** arise as a result of a geometrical change of the complexes *trans*- and *cis*-**4** rather than halide dissociation and formation of a pentacoordinate systems, as such a pentacoordinate complex would likely not be observed in strongly coordinating solvents such as MeCN.

Crystal structures of complexes *cis*-**6a** and *trans*-**7** were obtained and revealed both a distorted octahedral geometry around the rhodium center (Figure 2). While metal–ligand bond lengths are expected to alter according to the generally observed *trans* influence carbene > mesoionic carbene > phosphine > MeCN, complex *cis*-**6a** features the longer Rh–N_{MeCN} bond *trans* to the phosphine (2.125(3) Å) rather than *trans* to the carbene (2.098(3) Å; Table 2). Statistically, the difference is larger than 3 σ and thus significant, however the absolute difference of 0.03 Å may be governed by other than electronic effects such as crystal packing constrains. The Rh–C_{NHC} bond *trans* to phosphorus is 0.05 Å longer than the Rh–C_{NHC} bond *trans* to MeCN, which is conformal with the expected *trans* influence difference. Complex **7** shows considerably less distortion from octahedral geometry than

Scheme 2. Ligand Exchange Reactions Yielding Complexes 5, 6, and 7

Table 1. ^{31}P NMR Data for *cis* and *trans* Bidentate Dicarbene Rh(III) Complexes^a

	3a	4	5a	5a (CD ₃ CN)
<i>trans</i>	20.5 (75.2)	27.0 (75.1)	n.d.	28.6 (72.8)
<i>cis</i>	48.3 (116.6)	53.9 (123.7)	59.4 (122.4)	55.9 (120.6)
	20.8 (80.7)	28.7 (81.6)	44.3 (78.7)	40.8 (77.7)

^a δ_{P} in ppm (J_{PRh} in Hz in parentheses) in CD₂Cl₂ unless specified; n.d. = not determined.

complex 4, which can be quantified with the distortion index $\Sigma = 26.6^\circ$ for 7 and much higher for 4 ($\Sigma = 56.5^\circ$).²⁶ In addition, the Rh–C5 bond is 0.045 Å shorter in 7 than in 4, perhaps as consequence of both, the weaker *trans* influence of MeCN as compared to iodide and because of the reduced steric implications of MeCN relative to the larger iodide ligand. The variable bond lengths and angles of the tridentate C,C,C-

Table 2. Selected Bond Lengths (Å) and Angles (deg) for *cis*-6a and *trans*-7

	<i>cis</i> -6a	<i>trans</i> -7
Rh–C1	2.072(4)	2.027(2)
Rh–C9	2.021(3)	2.037(2)
Rh–P1	2.3618(9)	2.3475(5)
Rh–P2	2.2685(9)	2.3443(6)
Rh–N5	2.125(3)	2.085(2)
Rh–X ^a	2.098(3)	2.113(3)
C1–Rh–C9	87.04(14)	87.41(8)
C5–Rh–N5	–	171.03(7)
C1–Rh–P1	177.68(10)	176.13(7)

^aThe sixth ligand X in complex *cis*-6a is N6, in complex *trans*-7 X is C5 (see Figure 2).

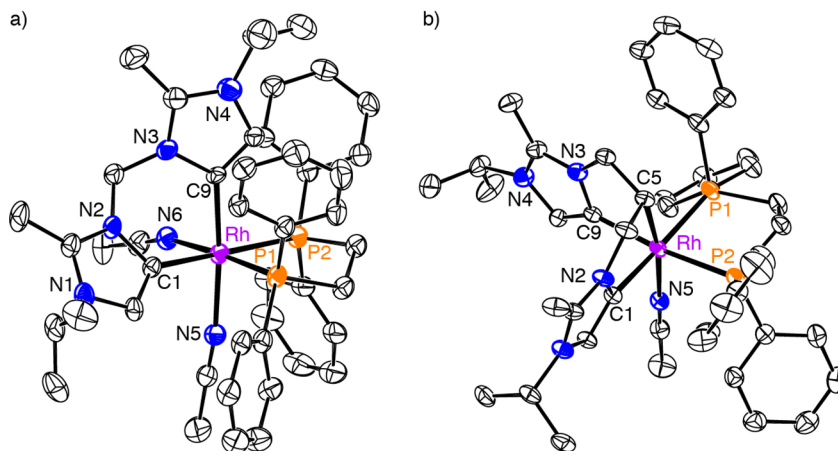


Figure 2. ORTEP representation of the cationic portion of (a) *cis*-6a and (b) *trans*-7 (50% probability ellipsoids; hydrogen atoms, counterions, and cocrystallized solvent molecules omitted for clarity).

dicarbene ligand in complexes **4** and **7** suggests some flexibility of this ligand scaffold.

Catalytic Transfer Hydrogenation. The new complexes **3–6** were used as precatalysts for the transfer hydrogenation of ketones.²⁷ Initially, benzophenone was used as a model substrate and activities were compared to complex **1**, which previously revealed substantial activity. The background base-induced reduction is poor giving only 8% of diphenylmethanol after 24 h (Table 3, entry 1). Complex **1a** is effective at low

Table 3. Catalytic Transfer Hydrogenation of Benzophenone with Rhodium(III) Dicarbene dppe Complexes 1–6^a

entry	[Rh]	mol % [Rh]	yield/%			TON
			0.5 h	2 h	24 h	
1	–	–	0	1	8	–
2	1a	0.15	26	50	82	550
3	3a	0.15	77	100	n.d.	670
4	3b	0.15	97	100	n.d.	670
5	4	0.15	10	23	71	470
6	5a	0.15	68	96	100	670
7	6a	0.15	10	25	59	390
8	6b	0.15	15	23	26	170
9	3a	0.05	39	55	78	1560
10	3b	0.05	36	76	94	1880
11	3a	0.01	4	7	22	2200
12	3b	0.01	0	3	18	1800
13	3b	0.01 ^b	21	33	46	4600

^aGeneral conditions: benzophenone (1.0 mmol), KOH (50 μ L, 2 M in H₂O, 0.1 mmol), *i*PrOH (5 mL), reflux temperature; yields determined by ¹H NMR spectroscopy, n.d. = not determined.

^bBenzophenone (10 mmol).

catalyst loadings (0.15 mol % [Rh]) although it does not reach full conversion even after 24 h (entry 2). The bidentate dicarbene diphosphine complexes **3a,b** afforded the most active catalysts of the series and gave complete conversion within 2 h at 0.15 mol % loading (entries 3, 4). For example, the turnover frequency at 50% conversion raised from TOF₅₀ = 330 h⁻¹ for **1a** up to TOF₅₀ > 1300 h⁻¹ upon introducing a phosphine ligand as in complex **3b** (TOF₅₀ > 1000 h⁻¹ for complex **3a**).²⁸ The chloride complex **5a** showed similar activity to the iodide analogue **3a**, in agreement with facile activation of the halide species with the in situ formed KO*i*Pr (entry 6). While previous work revealed higher performance for the chloro analogue of **1a**,^{17a} the introduction of a diphosphine ligand evidently reduces the influence of the halide on the catalytic activity. Sampling at early stages of a **3a**-catalyzed transfer hydrogenation indicates a fast catalyst activation and no significant induction period (Figure S1).²⁹

The tridentate C,C-dicarbene complex **4** was considerably less active than **3** presumably due to the availability of only one site for hydride formation (entry 5). Even after 24 h, full conversion was not reached and formation of a black precipitate pointed to the decomposition of the complex. The solvento complexes **6a,b** were unstable under the catalytic conditions and a dark precipitate formed within less than 30 min. These observations may rationalize the comparably poor conversions (entries 7,8), and they suggest that the heterogenized system is not efficient.

Conversions remained high when lowering the loadings of **3a,b** to 0.05 mol % (entries 9,10). Complex **3b**, with C2-phenyl and N-butyl substituents was the most robust system with turnover numbers (TON) up to 1880. A further decrease of the catalyst loading to 0.01 mol % resulted in a sharp decline in activity (entries 11,12). Even though the TONs remained in the low thousands conversion was prohibitively low. Increasing the substrate rather than lowering the catalyst loading to keep the 10,000:1 substrate/catalyst ratio improved the spectroscopic yield of the alcohol, and complex **3b** achieved TONs of almost 5000 (entry 13). This improvement constitutes one of the highest performances for rhodium(III) complexes in transfer hydrogenation.³⁰ The better performance at higher substrate loading may point to an adverse effect of minor impurities in the solvent when the concentration of the complex is too low.

Optimizations of the reaction conditions employing complexes **3a** and **3b** on focused on the use of the base as additive (Table 4). Standard conditions involved KOH as a

Table 4. Optimization Studies with Rhodium(III) Dicarbene dppe Complexes 3a and 3b^a

entry	[Rh]	mol % base	yield/%		
			0.5 h	2 h	24 h
1	3a	10	77	100	n.d.
2	3a	5	65	93	96
3	3a	1	6	9	9
4	3a	1 ^b	30	64	80
5	3b	10	97	100	n.d.
6	3b	5	84	100	n.d.
7	3b	1	21	37	39
8	3b	1 ^b	31	60	67

^aGeneral conditions as in Table 3, 0.15 mol % [Rh]. ^bWater (45 μ L) added.

base, which was added in 10 mol % with respect to the substrate as a 2 M aqueous solution. No reaction was observed in the absence of base or upon using NaOAc in the same molar ratio (0.1 mmol, 10 mol %) as a less corrosive base.³¹ Reducing the amount of KOH from 10 to 5 mol % lowered the catalytic rate slightly, though full conversion was readily achieved (entry 2). However, at 1 mol % base, activity was only marginal (entry 3). Since lowering the amount of KOH was also accompanied by a reduction of the aqueous fraction, a run was carried out using 1 mol % base (5 μ L of a 2 M solution) together with an additional amount of water (45 μ L) to achieve the same 100:1 *i*PrOH/H₂O ratio as in the runs performed with 10 mol % base. Under these conditions, the conversions improved substantially and reached up to 80% after 24 h (entry 4). While this beneficial effect of added water may be attributed to a bulk solvent effect, other factors may contribute, such as an enhanced polarity of the reaction medium to facilitate iodide dissociation or iodide stabilization to induce catalytic turnover. Such milder conditions may become attractive when corrosion or base-sensitivity of the substrate is an issue. Similar trends were observed for complex **3b**, and conversions with 1 mol % base were acceptable provided water was added to the reaction mixture (entries 5–8).

The substrate scope for transfer hydrogenation with **3b** was expanded to include other ketones and imines (Table 5).

Table 5. Catalytic Transfer Hydrogenation of Various Substrates with Complex **3b^a**

entry	substrate	product(s)	mol% 3b	Yield (%)		
				0.5 h	2 h	24 h
1			0.05	71	99	100
2			0.15	36	62	100
3			0.15	73	95	97
4			0.15	35	73	86
5			0.15	71	95	98
6			0.15	58	78	^b 84
7			0.15	<3	<3	<3
8		 	0.15	^c 19/11	23/11	n.d.
9		 	0.15	^d 45/0	22/65	0/97

^aGeneral conditions as in Table 3. ^b5 h. ^cYield shown as yield of I/II.

^dYield shown as III/IV.

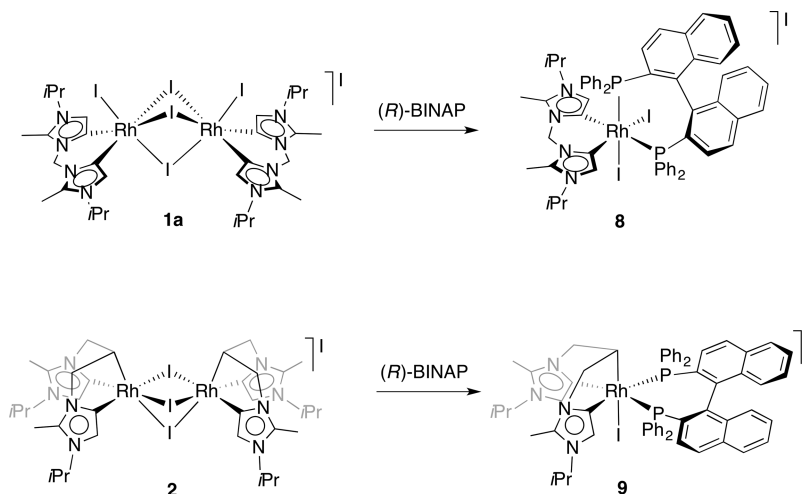
Cyclohexanone was fully reduced to cyclohexanol within 2 h at 0.05 mol % catalyst loading (2000 TON; entry 1), achieving a turnover frequency at 50% conversion, TOF₅₀ around 3000 h⁻¹. Hydrogenation of 2-acetylpyridine was slower than related aryl ketones but full conversion was reached within 24 h (entry 2). This substrate is usually challenging as both the substrate and the product alcohol are potentially chelating ligands that tend to poison the catalyst. In **3b**, the presence of chelating dicarbene and diphosphine ligands and their variable coordination modes (cf. isomerization, Scheme 1) presumably prevents such chelation and thus inhibits catalyst poisoning. Since the pyridyl unit was not deactivating the catalyst, imines were investigated as substrates. However, benzylidene

benzylidene (PhC=NCH₂Ph) was not converted. Likewise carbonyl groups of esters as in methyl benzoate were not hydrogenated, and instead base-induced saponification was observed in the presence of 10 mol % base. Classical substrates such as (substituted) acetophenone was transfer hydrogenated in good conversion (entries 3–6). The activity was moderately dependent on the electronic nature of the substituent, and in agreement with previous studies, electron-withdrawing substituents increase the electrophilicity of the carbonyl group and hence facilitate reduction.²⁷ Phenolic substrates such as 4-hydroxyacetophenone are not converted (entry 7), presumably because of the higher acidity of phenoles compared to *i*PrOH, thus preventing formation of the alkoxide that is presumed to be essential for ensuing β -hydrogen elimination and effective hydrogen transfer from *i*PrOH. Aldehydes are converted unselectively and produce the primary alcohol as well as benzylidene acetone (entry 8). Finally, enones with an α,β -unsaturated ketone functionality such as *trans*-chalcone were fully transfer hydrogenated with complex **3b**, and yielded the saturated alcohol due to transfer hydrogenation of the ketone and the olefin (24 h; entry 9). Samples taken after 30 min, i.e., at early conversion stages, revealed formation of the saturated ketone as the major product, suggesting a preference for the reduction of the olefinic C=C bond prior to ketone reduction. These results are in agreement with the selectivity observed for a NHC ruthenium(II) catalyst.³²

Synthesis of Dicarbene BINAP Rhodium(III) Complexes and Catalytic Activity. The facile coordination of dppe and the enhanced catalytic performance of the rhodium center when ligated by both dicarbene and diphosphine ligands provides a straightforward methodology for catalyst modification through variation of the phosphine. We have probed this approach by using the axially chiral BINAP ligand³³ which may afford a precatalyst with potential for asymmetric transfer hydrogenation reactions. Thus, heating the dinuclear rhodium complexes **1** and **2** in CH₂Cl₂ with (*R*)-BINAP yielded the rhodium complexes **8** and **9**, respectively, in moderate to good yields (52–74%; Scheme 3).

The pertinent NMR unambiguously evidenced coordination of BINAP to the rhodium center and revealed the specific ligand arrangement. Thus, the *cis* isomer of complex **8** was identified as the initial product by the two doublets of doublets centered at $\delta_P = 7.66$ (¹J_{PRh} = 119.7 Hz, ²J_{PP} = 20.3 Hz) and

Scheme 3. Synthesis of Dicarbene Binap Rhodium(III) Complexes **8 and **9****



1.04 ($^1J_{\text{PRh}} = 79.3$ Hz; CD_2Cl_2 solution). The Rh–P coupling constants were diagnostic and identified a weakly donating iodide *trans* to the low-field phosphine, while the smaller Rh–P coupling constant of the higher field resonance suggests a carbene in *trans* position.³⁴ Notably the imidazolylidene proton resonances are significantly separated in the ^1H NMR spectrum ($\delta_{\text{H}} = 7.33$ and 4.66) due to shielding of one of the protons by the naphthyl group of BINAP, thus further supporting an all-*cis* coordination.

Complex **8** isomerizes rapidly in CDCl_3 solution, and after 4 h, two new well resolved doublets of doublets emerged slightly downfield, at $\delta_{\text{P}} = 5.0$ and 9.0 for a new species, **8'** (3:1 ratio of **8**:**8'** after 4 h from an initial 25:1 ratio). The coupling constants for **8'** are very similar to those of the initially formed species **8**, thus indicating that one phosphorus remains *trans* to a carbene while the other phosphorus is *trans* to iodide.³⁵ In contrast to **8**, the NMR signals for **8'** are well resolved at room temperature. These data may indicate that the isomerization here arises due to an intraligand transformation, for example inversion of the metallacycle containing the NHC ligands. Again, the isomerization is slower in CD_2Cl_2 than in CDCl_3 and only traces of **8'** were observed after 6 h in solution, and about 30% after 3 weeks. No BINAP oxide was detected, indicating the complex is stable in solution at room temperature for extended periods.

While numerous attempts failed to crystallize complex **8**, single crystals suitable for X-ray diffraction analyses were obtained from the corresponding solvento complex. This complex was prepared by exchange of the iodide ligands with BF_4^- using AgBF_4 in MeCN.³⁶ The molecular structure confirmed the all *cis* ligand arrangement (Figure 3). The two

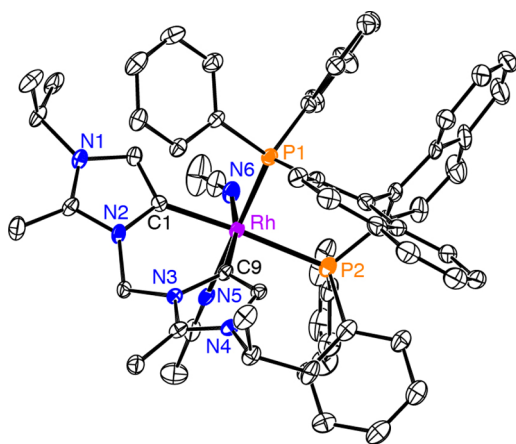


Figure 3. ORTEP representation of the solvento complex of **8** (50% probability ellipsoids; hydrogen atoms, BF_4^- counterions and cocrystallized solvent molecules omitted for clarity). Selected bond lengths (Å) and angles (deg): Rh–C1, 2.028(3), Rh–C9, 2.026(3), Rh–P1, 2.3091(7), Rh–P2, 2.4498(9), Rh–N5, 2.096(2); Rh–N6, 2.106(3); C1–Rh–C9, 86.97(14), C1–Rh–P2, 174.70(9).

Rh– C_{NHC} bond lengths are identical even though one carbene is *trans* to phosphorus and the other is *trans* to MeCN (cf. X-ray data for *trans*-**6a**). In contrast, the Rh–P bond *trans* to the carbene is a substantial 0.14 Å longer than the Rh–P bond *trans* to MeCN (2.4498(9) vs 2.3091(7) Å). Finally, the two Rh– N_{MeCN} bonds are essentially equally long (2.106(3) vs 2.096(2) Å). This latter comparison suggests that the *trans* influence of the phosphine and the carbene is not hugely different, and that the Rh–P and Rh– C_{NHC} bond lengths are governed by sterical constraints imposed by chelation and phosphorus substituents,

and much less by *trans* influences. Interestingly, the imidazolylidene proton adjacent to C9 points toward a naphthyl ring of the BINAP ligand (H10– $\text{Cg}_{\text{Naphth}}$ 2.477 Å). With this short distance, ring current effects become relevant and presumably account for the substantial shielding of this proton in the ^1H NMR spectrum (vide supra, $\delta_{\text{H}} = 4.66$), suggesting that the crystallographically determined structure is also preserved in solution.

Complex **9** containing a BINAP ligand and a C,C,C-tridentate dicarbene ligand was stable and does not undergo any isomerization in solution. It is characterized by two well resolved doublets of doublets in the ^{31}P NMR spectrum at $\delta_{\text{P}} = 13.37$ ($^1J_{\text{PRh}} = 81.3$ Hz, $^2J_{\text{PP}} = 25.2$ Hz) and 0.56 ($^1J_{\text{PRh}} = 79.9$ Hz). While ^{31}P NMR analysis does not give conclusive evidence of the ligand arrangement due to the similar coupling constants imparted by the *trans* carbene carbon and the anionic alkyl carbon (cf. *cis*- and *trans*-**4**), the ^{13}C NMR signals provide strong support for a *trans* conformation of **9**. The carbene signals were well resolved and appeared as two distinct doublet of doublet of doublets centered at 153.0 and 150.0 ppm, each with a large C– P_{trans} coupling (>120 Hz) and a small *cis* coupling (~10 Hz) in addition to the coupling to the ^{103}Rh nucleus. Moreover, the rhodium-bound alkyl carbon appears as a doublet of triplets due to coupling with two *cis*-positioned phosphorus atoms ($^1J_{\text{CRh}} = 28.4$ Hz, $^2J_{\text{CP}} = 4$ Hz). Unlike complex **8**, the imidazolylidene protons in complex **9** appear at a similar field ($\delta_{\text{H}} = 6.98$ and 6.92).

Complexes **8** and **9** were tested as transfer hydrogenation catalysts under standard conditions and compared to the dppe analogue, complex **4** (Table 6). Complex **4** showed moderate

Table 6. Transfer Hydrogenation of 4-Fluoroacetophenone with Complexes **4**, **8** and **9**^a

entry	[Rh]	yield/% (% ee)		
		0.5 h	2 h	24 h
1	4	24 (7)	55 (2)	70 (9)
2	8	100 (4)	n.d.	n.d.
3	9	85 (4)	97 (6)	n.d.

^aGeneral conditions: 4-fluoroacetophenone (1 mmol), KOH (2 M, 50 μL , 0.1 mmol), *i*PrOH (5 mL), 0.15 mol % [Rh], reflux; n.d. = not determined; enantiomeric excess as % ee determined by chiral HPLC in parentheses.

activity toward 4-fluoroacetophenone, yielding 70% of the corresponding alcohol after 24 h (entry 1). Both **8** and **9** were substantially more active and gave complete conversion after 0.5 and 2 h, respectively (entries 2,3). Hence, BINAP accelerates the hydrogen transfer reaction compared to dppe. We speculatively attribute the increased catalytic activity to the enhanced rigidity of the BINAP ligand, which may facilitate substrate coordination in a putative five-coordinate active species. The enantiomeric excess (% ee) of the alcohol product was poor for each run, even when determined at low conversion (5 min). Hence, under the applied conditions no enantioselectivity was imparted by the BINAP ligand, likely because of the high reaction temperature.^{30d,37}

CONCLUSIONS

A series of mixed dicarbene diphosphine rhodium(III) complexes with different spectator ligands were synthesized and tested in transfer hydrogenation catalysis. The complexes display dynamic behavior in solution as indicated by the *cis/trans* isomerization. The formation of dppe oxide indicates some lability of dppe coordination in solution, which is presumably facilitated by the strong *trans* effect of the carbene donors. BINAP is more rigid in its coordination to rhodium and no BINAP oxide was formed in the same time frame. Incorporation of the diphosphine ligands increases the catalytic activity of the rhodium center compared to the precursor dicarbene rhodium(III) complexes. The process is robust and tolerates additional water and lowering of the base loading, and even difficult substrates, such as 2-acetylpyridine are efficiently converted to the hydrogenated product. When the halide anions were replaced for BF_4^- , the complexes were no longer stable under catalytically relevant conditions. Under the conditions tested BINAP does not impart any selectivity under the applied conditions but leads to higher catalytic activity of the C,C'-dicarbene rhodium(III) catalyst than dppe does.

EXPERIMENTAL SECTION

General Comments. Complexes **1a**, **1b**, **3b**, and **2**, were synthesized as reported in the literature.¹⁷ All other reagents were used as received from commercial suppliers. Unless specified, NMR spectra were recorded at 25 °C on Varian spectrometers operating at 400 or 500 MHz (^1H NMR), 100 MHz (^{13}C NMR) and 162 MHz (^{31}P NMR) respectively. Chemical shifts (δ in ppm, coupling constants J in Hz) were referenced to residual solvent signals (^1H , ^{13}C) or external H_3PO_4 (^{31}P). Assignments are based on homo- and heteronuclear shift correlation spectroscopy. Elemental analyses were performed at UCD Microanalytical Laboratory using an Exeter Analytical CE-440 elemental analyzer, residual solvent was confirmed by NMR spectroscopy and also by X-ray structure determinations. Gas chromatography was carried out on a Shimadzu GC-174 gas chromatograph equipped with an Agilent DB5 column (J&W, 30 m) and a diode array detector at 120 °C.

Complex 3a. Complex **1a** (200 mg, 0.134 mmol) and 1,2-bis(diphenylphosphino)ethane (122 mg, 0.306 mmol) were dissolved in dry CH_2Cl_2 (5 mL) and stirred at room temperature for 19 h. The reaction mixture was filtered through Celite and eluted with CH_2Cl_2 (100 mL). After solvent evaporation, the residue was purified by gradient column chromatography (SiO_2 ; CH_2Cl_2 then CH_2Cl_2 /acetone, 1:1) affording complex **3a** as a mixture of two isomers (215 mg, 70%). Spectroscopic data of *trans*-**3a**: ^1H NMR (CD_2Cl_2 , 400 MHz): δ 7.65–7.60 (m, 8H, H_{phenyl}), 7.40–7.33 (m, 12H, H_{phenyl}), 7.02 (s, 2H, NCH_2N), 6.62 (s, 2H, H_{imid}), 4.41 (septet, 2H, $^3J_{\text{HH}} = 6.6$ Hz, $\text{NCH}(\text{Me})_2$), 3.19–3.13 (m, 4H, $\text{PC}_2\text{H}_4\text{P}$) 3.03 (s, 6H, $\text{C}_{\text{imid}}-\text{CH}_3$), 1.31 (d, 12H, $^3J_{\text{HH}} = 6.6$ Hz, $\text{NCH}(\text{CH}_3)_2$). $^{13}\text{C}\{^1\text{H}\}$ NMR (CD_2Cl_2 , 100 MHz): δ 140.9 (m, $\text{NC}_{\text{imid}}\text{N}$), 134.9 (C–Rh, $^1J_{\text{CRh}} = 32.8$ Hz, $^2J_{\text{CPcis}} = 9.7$ Hz, $^2J_{\text{CPtrans}} = 147$ Hz), 134.3 ($\text{C}_{\text{ipso}} + \text{C}_{\text{ortho}}$), 130.6 (C_{para}), 128.1 (C_{meta}), 125.9 ($\text{C}_{\text{imid}}-\text{H}$, $^3J_{\text{CP}} = 8.5$ Hz), 62.1 (NCH_2N), 50.4 ($\text{NCH}(\text{Me})_2$), 28.1 ($\text{PC}_2\text{H}_4\text{P}$), 23.0 ($\text{NCH}(\text{CH}_3)_2$), 12.8 ($\text{C}_{\text{imid}}-\text{CH}_3$). $^{31}\text{P}\{^1\text{H}\}$ NMR (CD_2Cl_2 , 162 MHz): δ 20.5 (d, $^1J_{\text{PRh}} = 75.2$ Hz). Spectroscopic data of *cis*-**3a**: ^1H NMR (CD_2Cl_2 , 400 MHz): δ 8.14–8.10 (m, 2H, H_{phenyl}), 8.02–7.97 (m, 2H, H_{phenyl}), 7.52–7.47 (m, 4H, H_{phenyl}), 7.28–7.19 (m, 8H, H_{phenyl}), 6.56 (s, 1H, H_{imid}), 4.63 (s, 1H, H_{imid}), 3.85 (septet, 1H, $^3J_{\text{HH}} = 6.7$ Hz, $\text{NCH}(\text{Me})_2$), 3.57 (m, 2H, $\text{NCH}(\text{Me})_2$ and $\text{PC}_2\text{H}_4\text{P}$), 2.54 (s, $\text{C}_{\text{imid}}-\text{CH}_3$), 0.62, 0.34 ($2 \times \text{d}$, $^3J_{\text{HH}} = 6.7$ Hz, $\text{NC}(\text{CH}_3)_2$). $^{31}\text{P}\{^1\text{H}\}$ NMR (CD_2Cl_2 , 162 MHz): δ 48.3 (dd, $^1J_{\text{PRh}} = 116.6$ Hz, $^2J_{\text{PP}} = 7.3$ Hz), 20.8 (dd, $^1J_{\text{PRh}} = 80.7$ Hz, $^2J_{\text{PP}} = 7.3$ Hz). ESI-MS (m/z): 1015.0544, calcd for [(dicarb) (dppe)-(I) $_2$ Rh] $^+$ 1015.0499. Anal. calcd for $\text{C}_{41}\text{H}_{48}\text{I}_3\text{N}_4\text{P}_2\text{Rh}$ (1142.41 g

$\text{mol}^{-1}) \times \text{CH}_2\text{Cl}_2$: C, 41.13; H, 3.84; N, 4.21. Found: C, 41.10; H, 4.11; N, 4.56.

Complex 4. Complex **2** (203 mg, 0.158 mmol) and 1,2-bis(diphenylphosphino)ethane (126 mg, 0.316 mmol) were dissolved in dry CH_2Cl_2 (5 mL) and stirred at room temperature for 19 h. The reaction mixture was filtered through Celite and eluted with CH_2Cl_2 (100 mL). After solvent evaporation, the residue was purified by gradient column chromatography (SiO_2 ; CH_2Cl_2 then CH_2Cl_2 /acetone, 1:2) yielding the title complex as a mixture of four isomers (270 mg, 82%, 2:1:0.4:0.15). Crystals of **4** were obtained by slow diffusion of Et_2O onto a CH_2Cl_2 solution of the complex. Spectroscopic data of *cis*-**4**: ^1H NMR (CD_2Cl_2 , 400 MHz): δ 8.01 (t, 2H, $^3J_{\text{HH}} = 8.5$ Hz, H_{phenyl}), 7.87–7.79 (m, 2H, H_{phenyl}), 7.71 (t, 2H, $^3J_{\text{HH}} = 8.2$ Hz, H_{phenyl}), 7.52–7.19 (m, 8H, H_{phenyl}), 7.10–7.02 (m, 4H, H_{phenyl}), 6.86 (t, 2H, $^3J_{\text{HH}} = 8.3$ Hz, H_{phenyl}), 6.59 (s, 1H, H_{imid}), 4.76 (dd, 1H, $^2J_{\text{HH}} = 12.2$ Hz, $^3J_{\text{HH}} = 7.0$ Hz, NCH_2), 4.36 (s, 1H, H_{imid}), 4.32–4.23 (m, 2H, NCH_2 and $\text{NCH}(\text{Me})_2$), 4.15–3.90 (m, 2H, NCH_2 and $\text{NCH}(\text{Me})_2$), 3.79 (dd, 1H, $^2J_{\text{HH}} = 12.9$ Hz, $^3J_{\text{HH}} = 8.8$ Hz, NCH_2), 3.08–2.63 (m, 5H, $\text{PC}_2\text{H}_4\text{P}$ and RhCH), 2.30 (s, 3H, $\text{C}_{\text{imid}}-\text{CH}_3$), 2.25 (s, 3H, $\text{C}_{\text{imid}}-\text{CH}_3$), 1.48, 1.33, 0.98, 0.92 ($4 \times \text{d}$, 3H , $^3J_{\text{HH}} = 6.6$ Hz, $\text{NCH}(\text{CH}_3)_2$). $^{13}\text{C}\{^1\text{H}\}$ NMR (CD_2Cl_2 , 100 MHz): δ 152 ($\text{C}_{\text{imid}}-\text{Rh}$), 38 150 ($\text{C}_{\text{imid}}-\text{Rh}$), 38 137.8 ($\text{NC}_{\text{imid}}\text{N}$), 137.0 ($\text{NC}_{\text{imid}}\text{N}$), $^4J_{\text{CP}} = 1.2$ Hz), 136.4–128.0 (C_{phenyl}), 118.8, 115.6 ($2 \times \text{C}_{\text{imid}}-\text{H}$), 62.0 (NCH_2 , $^3J_{\text{CP}} = 6.0$ Hz), 58.7 (NCH_2 , $^3J_{\text{CP}} = 5.6$ Hz), 49.7, 48.9 ($2 \times \text{NCH}(\text{Me})_2$), 36.7 ($\text{C}_{\text{alkyl}}-\text{Rh}$, $^1J_{\text{CRh}} = 20.9$ Hz, $^2J_{\text{CPtrans}} = 93.0$ Hz, $^2J_{\text{CPcis}} = 5.5$ Hz), 28.9, 26.8 ($2 \times \text{PCH}_2$), 23.9, 23.3, 23.1, 22.6 ($4 \times \text{NCH}(\text{CH}_3)_2$), 12.3, 12.2 ($2 \times \text{C}_{\text{imid}}-\text{CH}_3$). $^{31}\text{P}\{^1\text{H}\}$ NMR (CD_2Cl_2 , 162 MHz): δ 35.9 (dd, $^1J_{\text{PRh}} = 78.3$ Hz, $^2J_{\text{PP}} = 3.5$ Hz), 31.27 (dd, $^1J_{\text{PRh}} = 82.0$ Hz, $^2J_{\text{PP}} = 3.5$ Hz). Spectroscopic data for *trans*-**5**: ^1H NMR (CD_2Cl_2 , 400 MHz): δ 7.22 (s, 2H, H_{imid}), 2.62 (s, 6H, $\text{C}_{\text{imid}}-\text{CH}_3$), 1.50–1.40 (m, 12H, $\text{NCH}(\text{CH}_3)_2$), other signals overlapping with *cis*-**4**. $^{31}\text{P}\{^1\text{H}\}$ NMR (CD_2Cl_2 , 162 MHz): δ 28.9 (d, $^1J_{\text{PRh}} = 83.7$ Hz). ESI-MS (m/z): 915.1644, calcd for [(C,C'-dicarb) (dppe)(I)Rh] $^+$ 915.1689. Anal. calcd for $\text{C}_{43}\text{H}_{51}\text{I}_2\text{N}_4\text{P}_2\text{Rh}$ (1042.55 g mol^{-1}): C, 49.54; H, 4.93; N, 5.37. Found: C, 49.41; H, 4.99; N, 4.98.

Complex 5a. Complex **3a** (185 mg, 0.162 mmol) was dissolved in 1,2-dichloroethane (10 mL) and refluxed for 24 h. The product was precipitated with Et_2O (50 mL) and isolated by centrifugation. After solvent evaporation complex **5a** was isolated as a mixture of two isomers (137 mg, 97%) in a 1:0.3 ratio. Spectroscopic data for *cis*-**5a**: ^1H NMR (CD_2Cl_2 , 400 MHz): δ 8.22–8.17 (m, 2H, H_{phenyl}), 7.99–7.95 (m, 2H, H_{phenyl}), 7.43–7.24 (m, 14H, H_{phenyl}), 7.08 (d, 1H, $^2J_{\text{HH}} = 12.1$ Hz, lowfield AB part of NCH_2N), 6.64–6.60 (m, 2H, H_{phenyl}), 6.55 (d, 1H, $^2J_{\text{HH}} = 12.1$ Hz, highfield AB part of NCH_2N), 6.08 (s, 1H, H_{imid}), 4.60 (s, 1H, H_{imid}), 4.48–4.34 (m, 1H, $\text{NCH}(\text{Me})_2$), 3.89 (septet, 1H, $^3J_{\text{HH}} = 6.5$ Hz, $\text{NCH}(\text{Me})_2$), 3.47–3.29 (m, 2H, PCH_2), 3.08–2.93 (m, 5H, CH_2P and $\text{C}_{\text{imid}}-\text{CH}_3$), 2.85 (s, 3H, $\text{C}_{\text{imid}}-\text{CH}_3$), 1.23 (m, 6H, $\text{NC}(\text{CH}_3)_2$), 0.58, 0.42 ($2 \times \text{d}$, 3H , $^3J_{\text{HH}} = 6.5$ Hz, $\text{NC}(\text{CH}_3)_2$). $^{13}\text{C}\{^1\text{H}\}$ NMR (CD_2Cl_2 , 100 MHz): δ 141.3 ($\text{NC}_{\text{imid}}\text{N}$), $^4J_{\text{CP}} = 5.3$ Hz), 141.0 ($\text{C}_{\text{imid}}-\text{Rh}$, $^1J_{\text{CRh}} = 33.1$ Hz, $^2J_{\text{CPcis}} = 13.0$ Hz, $^2J_{\text{CPtrans}} = 149.5$ Hz), 140.0 ($\text{NC}_{\text{imid}}\text{N}$), 135.4 ($\text{C}_{\text{imid}}-\text{Rh}$, $^1J_{\text{CRh}} = 40.3$ Hz, $^2J_{\text{CP}} = 9.0$ Hz), 134.7–127.8 (C_{phenyl}), 122.1 ($\text{C}_{\text{imid}}-\text{H}$, $^3J_{\text{CP}} = 8.9$ Hz, $^3J_{\text{CP}} = 4.5$ Hz), 121.3 ($\text{C}_{\text{imid}}-\text{H}$, $J = 8.3$ Hz, $J = 3.4$ Hz), 59.3 (NCH_2N), 50.3, 49.6 ($2 \times \text{NCH}(\text{Me})_2$), 28.4 (PCH_2 , $^1J_{\text{CP}} = 17.3$ Hz), 28.0 (CH_2P , $^1J_{\text{CP}} = 17.5$ Hz), 23.2, 22.4, 22.37, 22.0 ($4 \times \text{NC}(\text{CH}_3)_2$), 12.8, 12.4 ($2 \times \text{C}_{\text{imid}}-\text{CH}_3$). $^{31}\text{P}\{^1\text{H}\}$ NMR (CD_2Cl_2 , 162 MHz): δ 53.9 (dd, $^1J_{\text{PRh}} = 123.7$ Hz, $^2J_{\text{PP}} = 10.3$ Hz), 28.7 (dd, $^1J_{\text{PRh}} = 81.6$ Hz, $^2J_{\text{PP}} = 10.3$ Hz). Spectroscopic data for *trans*-**5a**: ^1H NMR (CD_2Cl_2 , 400 MHz): δ 7.61–7.54 (m, 8H, H_{phenyl}), 7.43–7.24 (m, 12H, H_{phenyl}), 6.47 (s, 2H, H_{imid}), 4.48–4.34 (m, 2H, $\text{NCH}(\text{Me})_2$), 3.0–2.8 ($\text{PC}_2\text{H}_4\text{P}$), 2.87 (s, 6H, $\text{C}_{\text{imid}}-\text{CH}_3$), 1.36 (d, 6H, $^3J_{\text{HH}} = 6.5$ Hz). Reminding signals overlapping with the *cis* isomer. $^{13}\text{C}\{^1\text{H}\}$ NMR (CD_2Cl_2 , 100 MHz): δ 140.8 (m, $\text{NC}_{\text{imid}}\text{N}$), 138.7 ($\text{C}_{\text{imid}}-\text{Rh}$, $^1J_{\text{CRh}} = 32.6$ Hz, $^2J_{\text{CPcis}} = 9.9$ Hz, $^2J_{\text{CPtrans}} = 150.0$ Hz), 134.7–127.8 (C_{phenyl}), 124.7 ($\text{C}_{\text{imid}}-\text{H}$, $^3J_{\text{CP}} = 8.6$ Hz), 59.1 (NCH_2N), 50.2 ($\text{NCH}(\text{Me})_2$), 27.1 (m, $\text{PC}_2\text{H}_4\text{P}$), 22.6 ($\text{NCH}(\text{CH}_3)_2$), 11.8 ($\text{C}_{\text{imid}}-\text{CH}_3$). $^{31}\text{P}\{^1\text{H}\}$ NMR (CD_2Cl_2 , 160 MHz): δ 27.0 (d, $^1J_{\text{PRh}} = 75.1$ Hz). ESI-MS (m/z): 831.1770, calcd for [(dicarb) (dppe) (Cl) $_2$ Rh] $^+$ 831.1786. Anal. calcd for

$C_{41}H_{48}Cl_3N_4P_2Rh$ (868.06 g mol⁻¹) × 4 CH₂Cl₂: C, 44.75; H, 4.67; N, 4.64. Found: C, 44.79; H, 4.36; N, 5.02.

Complex 6a. Complex **3a** (73 mg, 0.064 mmol) and AgBF₄ (50 mg, 0.257 mmol) were dissolved in MeCN (10 mL) and stirred in the absence of light at room temperature for 18 h. A yellow suspension formed and was filtered through Celite. After removing all volatiles under reduced pressure, complex **6a** was obtained as a mixture of two isomers (71 mg, quantitative). Crystals suitable for X-ray diffraction studies were obtained by slow diffusion of Et₂O onto a CH₂Cl₂/MeCN (1:1) solution of the complex. Spectroscopic data³⁹ for *trans*-**6a**: ¹H NMR (CD₃CN, 400 MHz): δ 7.78–7.36 (m, 20H, H_{phenyl}), 6.26 (s, 2H, H_{imid}), 6.27 (d, 1H, ²J_{HH} = 13.9 Hz, lowfield AB part of NCH₂N), 5.90 (d, 1H, ²J_{HH} = 13.9 Hz, highfield AB part of NCH₂N), 4.49 (septet, 2H, ³J_{HH} = 6.4 Hz, NCHMe₂), 3.87–2.88 (m, 4H, PC₂H₄P), 2.74 (s, 6H, C_{imid}-CH₃), 1.34, 1.14 (2 × d, 6H, ³J_{HH} = 6.4 Hz, NCH(CH₃)₂). ¹³C{¹H} NMR (CD₃CN, 100 MHz): δ 143.8 (NC_{imid}N), ⁴J_{CP} = 4.6 Hz, 134.7–128.1 (C_{phenyl}), 134 (C_{imid}-Rh),³⁸ 124.6 (m, C_{imid}-H), 58.9 (NCH₂N), 50.7 (NCH(Me)₂), 27.4 (m, PC₂H₄P), 22.9, 22.3 (NCH(CH₃)₂), 10.6 (C_{imid}-CH₃). ³¹P{¹H} NMR (CD₃CN, 162 MHz): δ 28.6 (d, ¹J_{PRh} = 72.8 Hz). Spectroscopic data for *cis*-**6a**: ¹H NMR (CD₃CN, 400 MHz): δ 7.78–7.36 (m, 14H, H_{phenyl}), 7.34–7.28 (m, 2H, H_{phenyl}), 7.25–7.17 (m, 2H, H_{phenyl}), 6.75–6.67 (m, 2H, H_{phenyl}), 6.36 (d, 1H, ²J_{HH} = 14.0 Hz, lowfield AB part of NCH₂N), 5.93 (d, 1H, ²J_{HH} = 14.0 Hz, highfield AB part of NCH₂N), 5.56 (s, 1H, H_{imid}), 5.06 (s, 1H, H_{imid}), 4.55–4.47 (m, 1H, NCHMe₂), 4.06 (septet, 1H, ³J_{HH} = 6.6 Hz, NCHMe₂), 3.87–2.88 (m, 4H, PC₂H₄P), 2.83, 2.66 (2 × s, 3H, C_{imid}-CH₃), 1.25, 0.87, 0.58, 0.46 (4 × d, 3H, ³J_{HH} = 6.6 Hz, NCH(CH₃)₂). ¹³C{¹H} NMR (CD₃CN, 100 MHz): δ 145.3 (NC_{imid}N), 143.3 (NC_{imid}N), 134.7–128.1 (C_{phenyl}), 133 (C_{imid}-Rh),³⁸ 126 (C_{imid}-Rh),³⁸ 124.6 (C_{imid}-H), 122.5 (C_{imid}-H), 59.6 (NCH₂N), 51.1, 50.7 (2 × NCH(Me)₂), 27.4 (PC₂H₄P), 22.5, 22.1, 21.8, 21.7 (4 × NCH(CH₃)₂), 11.1, 10.6 (2 × C_{imid}-CH₃). ³¹P{¹H} NMR (CD₃CN, 162 MHz): δ 55.9 (dd, ¹J_{PRh} = 120.6 Hz, ²J_{PP} = 9.7), 40.8 (dd, ¹J_{PRh} = 77.7 Hz, ²J_{PP} = 9.7 Hz). ESI-MS (*m/z*): 380.6226, calcd for [(dicarb) (dppe)Rh]²⁺ 380.6205.

Complex 6b. Complex **3b** (0.060 g, 0.046 mmol) and AgBF₄ (0.050 g, 0.185 mmol) were dissolved in MeCN (10 mL) and stirred in the dark at room temperature for 2 h. The yellow suspension was filtered through Celite and all volatiles were removed under reduced pressure, yielding complex **6b** as a mixture of two isomers (0.58 g, quantitative). Spectroscopic data³⁹ for *trans*-**6b**: ¹H NMR (CD₃CN, 400 MHz): δ 7.86–7.36 (m, 26H, H_{phenyl}), 7.22–7.09 (m, 2H, H_{phenyl}), 6.77–6.70 (m, 2H, H_{phenyl}), 6.05 (s, 1H, H_{imid}), 5.96 (d, 1H, ³J_{HH} = 14.0 Hz, lowfield AB part of NCH₂N), 5.66 (d, 1H, ³J_{HH} = 14.0 Hz, highfield AB part of NCH₂N), 5.43 (s, 1H, H_{imid}), 3.91–3.70 (m, 2H, NCH₂), 3.85–3.75, 3.71–3.49, 3.39–3.26 (3 × m, 1H, PCH₂), 3.23–3.09 (m, 1H, NCH₂), 3.17–3.06 (m, 1H, PCH₂), 2.99–2.90 (m, 1H, NCH₂), 1.51–1.40, 1.13–0.99 (2 × m, 2H, NCH₂CH₃), 0.85–0.76, 0.75–0.72 (2 × m, 2H, CH₂CH₃), 0.72–0.70, 0.57–0.52 (2 × m, 3H, CH₂CH₃). ¹³C{¹H} NMR (CD₃CN, 100 MHz): δ 146.3 (NC_{imid}N), ⁴J_{CP} = 4.2 Hz, 144.5 (NC_{imid}N), 135 (C_{imid}-Rh),³⁸ 134.9–121.35 (C_{phenyl}), 129.8 (C_{imid}-H), 128 (C_{imid}-Rh),³⁸ 127.6 (C_{imid}-H), 60.0 (NCH₂N), 48.8, 48.2 (2 × NCH₂), 32.3, 32.2 (2 × NCH₂CH₃), 29.2 (PCH₂), 22.0 (CH₂P), 19.9, 19.4 (2 × CH₂CH₃), 13.4, 13.3 (2 × CH₂CH₃). ³¹P{¹H} NMR (CD₃CN, 162 MHz): δ 55.8 (dd, ¹J_{PRh} = 119.5 Hz, ²J_{PP} = 9.0 Hz), 44.2 (dd, ¹J_{PRh} = 79.0 Hz, ²J_{PP} = 9.0 Hz). Selected spectroscopic data for *trans*-**6b**: ¹H NMR (CD₃CN, 400 MHz): δ 7.72–7.35 (m, 30H, H_{phenyl}), 6.46 (s, 2H, H_{imid}), 5.91 (d, 1H, ³J_{HH} = 14.0 Hz, NCH₂N), 5.83 (br, 1H, NCH₂N), 3.80–3.75 (m, 4H, NCH₂), 3.63–3.46 (br, 2H, PCH₂), 3.23–3.06 (br, 2H, CH₂P), 1.53–1.41 (m, 4H, NCH₂CH₃), 1.15–1.03 (m, 4H, CH₂CH₃), 0.73 (t, 6H, ³J_{HH} = 7.0 Hz, CH₂CH₃). ³¹P{¹H} NMR (CD₃CN, 162 MHz): δ 30 (br d, ¹J_{PRh} = 71 Hz). ESI-MS (*m/z*): 456.6608, calcd for [(dicarb) (dppe)Rh]²⁺ 456.6517.

Complex 7. Complex **4** (101 mg, 0.097 mmol) and AgBF₄ (57 mg, 0.291 mmol) were dissolved in MeCN (5 mL) and stirred at room temperature for 2 h under exclusion of light. The reaction mixture was filtered through Celite and eluted with MeCN (20 mL) yielding the title complex as a mixture of four isomers (97 mg, quantitative). Crystals suitable for X-ray diffraction studies were obtained by slow

diffusion of Et₂O onto a CH₂Cl₂ solution of the isomeric mixture. Spectroscopic data of *cis*-**7**: ¹H NMR (CD₃CN, 400 MHz): δ 7.92–7.81 (m, 2H, H_{phenyl}), 7.74–7.68 (m, 2H, H_{phenyl}), 7.66–7.23 (m, 12H, H_{phenyl}), 7.21–7.15 (m, 1H, H_{phenyl}), 7.06 (t, 2H, ³J_{HH} = 8.6 Hz, H_{phenyl}), 6.99–6.92 (m, 1H, H_{phenyl}), 6.80 (s, 1H, H_{imid}), 5.09 (s, 1H, H_{imid}), 4.48–4.36 (m, 1H, NCHMe₂), 4.21–4.12 (m, 1H, NCH₂), 3.99 (septet, 1H, ³J_{HH} = 6.6 Hz, NCHMe₂), 3.56–3.46 (m, 1H, NCH₂), 3.45–3.13 (m, 4H, PC₂H₄P), 3.12–3.05 (m, 1H, NCH₂), 2.55 (s, 3H, C_{imid}-CH₃), 2.16–2.11 (m, 1H, NCH₂), 1.95 (s, 3H, C_{imid}-CH₃), 1.41, 1.35, 1.04, 0.92 (4 × d, 3H, ³J_{HH} = 6.6 Hz, NCH(CH₃)₂), CH-Rh not detected. ¹³C{¹H} NMR (CD₃CN, 100 MHz): δ 140.4 (NC_{imid}N), 138.8 (NC_{imid}N), 134.3–129.3 (C_{phenyl}), 120.7 (C_{imid}-H, ³J_{CP} = 13.0 Hz, ³J_{CP} = 3.6 Hz), 117.7 (C_{imid}-H), 59.7, 59.6 (2 × NCH₂), 50.2, 49.5 (2 × NCH(CH₃)₂), 36.8 (CH-Rh), 25.3 (PC₂H₄P), 22.8, 22.7, 22.4, 22.2 (4 × NCH(CH₃)₂), 11.6, 10.5 (2 × C_{imid}-CH₃), C_{imid}-Rh not resolved. ³¹P{¹H} NMR (CD₃CN, 162 MHz): δ 38.9 (dd, ¹J_{PRh} = 76.5 Hz, ²J_{PP} = 5.1 Hz), 35.6 (dd, ¹J_{PRh} = 82.6 Hz, ²J_{PP} = 5.1 Hz). Spectroscopic data of *trans*-**7**: ¹H NMR (CD₃CN, 400 MHz): δ 7.65–7.40 (20H, H_{phenyl}), 7.11 (s, 2H, H_{imid}), 4.48–4.36 (m, 2H, NCHMe₂), 2.09 (s, 6H, C_{imid}-CH₃), 1.54, 1.46 (2 × d, 6H, ³J_{HH} = 6.6 Hz, NCH(CH₃)₂). ¹³C{¹H} NMR (CD₃CN, 100 MHz): δ 139.7 (br, NC_{imid}N), 134.3–129.3 (C_{phenyl}), 117.1 (C_{imid}-H, ³J_{CP} = 7.9 Hz, ³J_{CP} = 2.7 Hz), 50.4 (NCH(CH₃)₂), 23.6, 22.2 (NCH(CH₃)₂), 10.9 (C_{imid}-CH₃). ³¹P{¹H} NMR (CD₃CN, 162 MHz): δ 32.6 (d, ¹J_{PRh} = 83.6 Hz), other signals overlapping with *cis*-**7** and not resolved. *Minor species*: ³¹P{¹H} NMR (CD₃CN, 121 MHz): δ 57.3 (d, ¹J_{PRh} = 133.0 Hz); 51.7 (dd, ¹J_{PRh} = 133.8 Hz, ²J_{PP} = 7.2 Hz), 35.7 (dd, ¹J_{PRh} = 74.6 Hz, ²J_{PP} = 7.2 Hz). Anal. calcd for C₄₅H₅₄B₂F₈N₈P₂Rh (1003.41 g mol⁻¹) × 1.25 CH₂Cl₂: C, 50.06; H, 5.13; N, 6.31. Found: C, 50.04; H, 4.87; N, 5.95.

Complex 8. Complex **1a** (100 mg, 0.067 mmol) and (*R*)-(+)-2,2'-bis(diphenylphosphino)-1,1'-binaphthalene (55 mg, 0.087 mmol) were dissolved in dry CH₂Cl₂ (5 mL) and stirred at 50 °C for 18 h under a nitrogen atmosphere. After evaporation of all volatiles, the residue was purified by gradient column chromatography (SiO₂; CH₂Cl₂ then CH₂Cl₂/acetone, 1:2), which gave orange complex **8** as a mixture of two isomers (95 mg, 52%, 97:3). Spectroscopic data of *cis*-**8**: ¹H NMR (CD₂Cl₂, 400 MHz): δ 8.55–8.33 (br, 2H, H_{aryl}), 7.91–7.11 (m, 21H, H_{aryl}), 7.33 (s, 1H, H_{imid}), 6.99 (d, 1H, ²J_{HH} = 12.9 Hz, lowfield AB part of NCH₂N), 6.88–6.40 (m, 7H, H_{aryl}), 6.29 (d, 1H, ²J_{HH} = 12.9 Hz, highfield AB part of NCH₂N), 5.76–5.70 (m, 2H, H_{aryl}), 4.66 (s, 1H, H_{imid}), 4.34 (septet, 1H, ³J_{HH} = 6.7 Hz, NCHMe₂), 4.02 (septet, 1H, ³J_{HH} = 6.7 Hz, NCHMe₂), 3.22, 2.66 (2 × s, 3H, C_{imid}-CH₃), 1.33, 1.20, 1.16, 0.73 (4 × d, 3H, ³J_{HH} = 6.7 Hz, NCH(CH₃)₂). ¹³C{¹H} NMR (CD₂Cl₂, 100 MHz): δ 142.6 (NC_{imid}N), 141.7 (C_{aryl}, ¹J_{CP} = 3.1 Hz), 141.6 (C_{aryl}, ¹J_{CP} = 3.0 Hz), 139.8–125.4 (C_{aryl}), 139.8 (NC_{imid}N), ⁴J_{CP} = 5.5 Hz, 129 (C_{imid}-H),³⁸ 125.5 (C_{imid}-H, ³J_{CP} = 6.9 Hz, ³J_{CP} = 3.3 Hz), 62.4 (NCH₂N), 51.1, 50.6 (2 × NCHMe₂), 23.4, 22.8, 21.8, 21.0 (4 × NCH(CH₃)₂), 14.5, 12.8 (2 × C_{ipso}-CH₃); C_{imid}-Rh not resolved. ³¹P{¹H} NMR (CD₂Cl₂, 162 MHz): δ 7.7 (dd, ¹J_{PRh} = 119.7 Hz, ²J_{PP} = 20.3 Hz), 1.0 (dd, ¹J_{PRh} = 79.3 Hz, ²J_{PP} = 20.3 Hz). Selected spectroscopic data of *cis*-**8**: ³¹P{¹H} NMR (CD₂Cl₂, 162 MHz): δ 8.5 (dd, ¹J_{PRh} = 120.0 Hz, ²J_{PP} = 20.8 Hz), 5.0 (dd, ¹J_{PRh} = 76.8 Hz, ²J_{PP} = 20.8 Hz). ESI-MS (*m/z*): 1239.1154, calcd for [(dicarb) (dppe)(I₂)Rh]⁺ 1239.1125. Anal. calcd for C₅₉H₅₆I₂N₄P₂Rh (1366.0 g mol⁻¹) × 2.5 CH₂Cl₂: C, 46.78; H, 3.89; N, 3.55. Found: C, 47.13; H, 3.55; N, 3.71.

Complex 9. Complex **2** (117 mg, 0.091 mmol) and (*R*)-(+)-2,2'-bis(diphenylphosphino)-1,1'-binaphthalene (77 mg, 0.124 mmol) were dissolved in dry, degassed CH₂Cl₂ (5 mL) and stirred at 50 °C for 16 h. All volatiles were evaporated and the residue was purified by gradient column chromatography (SiO₂; CH₂Cl₂ then CH₂Cl₂/acetone, 1:2), yielding complex **9** as a dark red solid (170 mg, 74%). ¹H NMR (CDCl₃, 400 MHz): δ 8.28 (t, 1H, ³J_{HH} = 7.9 Hz, H_{aryl}), 8.21 (dd, 1H, ³J_{HH} = 8.7 Hz, ³J_{HH} = 6.4 Hz, H_{aryl}), 8.06 (t, 2H, ³J_{HH} = 8.7 Hz, H_{aryl}), 7.86 (d, 1H, ³J_{HH} = 8.6 Hz, H_{aryl}), 7.72 (d, 1H, ³J_{HH} = 8.8 Hz, H_{aryl}), 7.70–7.62 (m, 3H, H_{aryl}), 7.51 (d, 1H, ³J_{HH} = 8.1 Hz, H_{aryl}), 7.32–7.04 (m, 12H, H_{aryl}), 6.98 (br, 1H, H_{imid}), 6.95–6.89 (m, 1H, H_{aryl}), 6.92 (s, 1H, H_{imid}), 6.88–6.82 (m, 2H, H_{aryl}), 6.64 (t, 1H, ³J_{HH} = 8.4 Hz, H_{aryl}), 6.61–6.56 (m, 3H, H_{aryl}), 6.49 (t, 1H, ³J_{HH} = 8.2 Hz,

H_{aryl} , 5.82 (d, 1H, $^3J_{\text{HH}} = 8.2$ Hz, H_{aryl}), 5.59 (d, 1H, $^3J_{\text{HH}} = 8.4$ Hz, H_{aryl}), 4.70 (br, 1H, CH–Rh), 4.13–4.06 (m, 1H, NCH_2), 3.94 (septet, 1H, $^3J_{\text{HH}} = 6.6$ Hz, NCHMe_2), 3.84 (septet, 1H, $^3J_{\text{HH}} = 6.6$ Hz, NCHMe_2), 3.58–3.50 (m, 2H, NCH_2), 3.29–3.21 (m, 1H, NCH_2), 2.09, 2.02 (2 \times s, 3H, $\text{C}_{\text{imid}}\text{--CH}_3$), 1.30 (d, 3H, $^3J_{\text{HH}} = 6.6$ Hz, $\text{NCH}(\text{CH}_3)_2$), 1.26–1.23 (m, 6H, $\text{NCH}(\text{CH}_3)_2$), 1.21 (d, 3H, $^3J_{\text{HH}} = 6.6$ Hz, $\text{NCH}(\text{CH}_3)_2$). $^{13}\text{C}\{^1\text{H}\}$ NMR (CDCl_3 , 100 MHz): δ 153.0 ($\text{C}_{\text{imid}}\text{--Rh}$, $^1J_{\text{CRh}} = 37.5$ Hz, $^2J_{\text{CPtrans}} = 130$ Hz, $^2J_{\text{CPcis}} = 9.1$ Hz), 151.0 ($\text{C}_{\text{imid}}\text{--Rh}$, $^1J_{\text{CRh}} = 37.5$ Hz, $^2J_{\text{CPtrans}} = 125$ Hz, $^2J_{\text{CPcis}} = 12.4$ Hz), 143.5 (C_{aryl} , $^1J_{\text{CP}} = 3.8$ Hz), 143.3 (C_{aryl} , $^1J_{\text{CP}} = 3.8$ Hz), 137.6–125.2 (C_{aryl}), 136.6, 136.3 (2 \times $\text{NC}_{\text{imid}}\text{N}$), 121.1 ($\text{C}_{\text{imid}}\text{--H}$, $^3J_{\text{CP}} = 9.3$ Hz), 120.3 ($\text{C}_{\text{imid}}\text{--H}$, $^3J_{\text{CP}} = 10.8$ Hz), 59.4 (NCH_2 , $^3J_{\text{CP}} = 4.6$ Hz), 56.1 (NCH_2 , $^3J_{\text{CP}} = 3.8$ Hz), 50.0, 48.8 (2 \times NCHMe_2), 35.0 (CH–Rh, $^1J_{\text{CRh}} = 28.4$ Hz, $^2J_{\text{CP}} = 4.0$ Hz), 23.4, 23.0, 22.7, 22.5 (4 \times $\text{NCH}(\text{CH}_3)_2$), 12.2, 12.1 (2 \times $\text{C}_{\text{imid}}\text{--CH}_3$). $^{31}\text{P}\{^1\text{H}\}$ NMR (CDCl_3 , 162 MHz): δ 13.4 (dd, $^1J_{\text{PRh}} = 81.3$ Hz, $^2J_{\text{PP}} = 25.2$ Hz), 0.6 (dd, $^1J_{\text{PRh}} = 79.9$ Hz, $^2J_{\text{PP}} = 25.2$ Hz). ESI-MS (m/z): 1139.2308, calcd for [(C,C,C-dicarb) (binap)(I)Rh] $^+$ 1139.2315. Anal. calcd for $\text{C}_{61}\text{H}_{59}\text{I}_2\text{N}_4\text{P}_2\text{Rh}$ (1266.81 g mol^{-1}) \times 1.75 CH_2Cl_2 : C, 53.25; H, 4.45; N, 3.96. Found: C, 53.28; H, 4.40; N, 4.33.

Typical Procedure for Catalytic Transfer Hydrogenation. The precatalyst was added as a CH_2Cl_2 solution (0.6 mL, 2.3 mM, 1.5 μmol Rh) to the reaction flask and the solvent was evaporated to dryness by heating in an oil bath (110 $^\circ\text{C}$) for 0.5 h. The presence of residual CH_2Cl_2 completely inhibited catalytic activity. After evaporation of CH_2Cl_2 , *i*PrOH (5 mL) and KOH (2 M solution in H_2O , 50 μL , 0.1 mmol) were added and the mixture was refluxed for 10 min. Then the substrate (1.0 mmol) was added and aliquotes (ca. 0.1 mL) were taken at set times, diluted with cyclohexane (2 mL) and filtered through a short pad of Celite, which was washed with Et_2O (3 \times 2 mL). The combined organic layers were evaporated to dryness and analyzed by ^1H NMR spectroscopy and/or gas chromatography. Yields are an average of at least two runs. Enantiomeric excess was determined by HPLC using a chiral OBH column and heptane/ EtOH 95:5 as eluent mixture at a 0.5 mL min^{-1} flow rate.

Crystal Structure Determinations. Crystal data for *trans*-4, *cis*-6a, *trans*-7 and the solvento complex of 8 were collected using a Rigaku (former Agilent Technologies) Oxford Diffraction SuperNova A diffractometer fitted with an Atlas detector and using monochromated Mo $K\alpha$ radiation (0.71073 \AA) for *trans*-4 and solvento-8 or Cu $K\alpha$ (1.54184 \AA) for *cis*-6a and *trans*-7. A complete (for 7 and 8) or 5-fold redundant (for 4 and 6a) data set was collected, assuming that the Friedel pairs are not equivalent. The structures were solved by direct methods using SHELXS-97 and refined by full-matrix least-squares fitting on F^2 for all data using SHELXL-97.⁴⁰ Hydrogen atoms were added at calculated positions and refined by using a riding model. Anisotropic thermal displacement parameters were used for all nonhydrogen atoms. The solvents in *trans*-4 and *cis*-6a and some of the solvent in solvento-8 could not be modeled in terms of atomic sites. The SQUEEZE option as incorporated in PLATON⁴¹ was used to compensate for the spread electron density. Further crystallographic details are compiled in Tables S1 and S2. Crystallographic data (excluding structure factors) for all three complexes have been deposited with the Cambridge Crystallographic Data Centre as supplementary publication no. 1425815 (*trans*-4), 1425814 (*cis*-6a), CCDC 1425813 (*trans*-7), and 1425816 (8).

■ ASSOCIATED CONTENT

Supporting Information

The Supporting Information is available free of charge on the ACS Publications website at DOI: 10.1021/acs.organomet.5b00809.

Representative time–conversion profile for catalytic activity of complex 3a. (PDF)

Crystallographic data. (CIF)

■ AUTHOR INFORMATION

Corresponding Author

*Phone: +41316314644. E-mail: martin.albrecht@dcb.unibe.ch.

Notes

The authors declare no competing financial interest.

■ ACKNOWLEDGMENTS

We thank the European Research Council (StG 208651 and CoG 615653), Science Foundation Ireland (10/RFP/CHS2844) and the NUI Travel Scheme (scholarship to K.F.) for financial support.

■ REFERENCES

- (1) (a) de Vries, J. G.; Elsevier, C. J., Eds.; *The Handbook of Homogeneous Hydrogenation*; Wiley-VCH: Weinheim, Germany, 2008. (b) Glorius, F., Ed.; *N-Heterocyclic Carbenes in Transition-Metal Catalysis*, Topics in Organometallic Chemistry; Springer: Berlin, Germany, 2007. (c) Cazin, C. S. J., Ed.; *N-Heterocyclic Carbenes in Transition Metal Catalysis and Organocatalysis*; Springer: Berlin, Germany, 2011. (d) Díez-González, S., Ed.; *N-Heterocyclic Carbenes; From Laboratory Curiosities to Efficient Synthetic Tools*; RSC Catalysis Series: Cambridge, U.K., 2011. (e) Nolan, S. P., Ed.; *N-Heterocyclic Carbenes*; Wiley-VCH: Weinheim, Germany, 2014.
- (2) (a) Göttker-Schnetmann, I.; White, P.; Brookhart, M. J. *Am. Chem. Soc.* **2004**, *126*, 1804. (b) Crabtree, R. H. *J. Organomet. Chem.* **2004**, *689*, 4083.
- (3) (a) Vougioukalakis, G. C.; Grubbs, R. H. *Chem. Rev.* **2010**, *110*, 1746. (b) Monfette, S.; Fogg, D. E. *Chem. Rev.* **2009**, *109*, 3783. (c) Samojłowicz, C.; Bieniek, M.; Grela, K. *Chem. Rev.* **2009**, *109*, 3708.
- (4) (a) Díez-González, S.; Marion, N.; Nolan, S. P. *Chem. Rev.* **2009**, *109*, 3612. (b) Cornils, B.; Herrmann, W. A. *Applied Homogeneous Catalysis with Organometallic Compounds*; Wiley-VCH: Weinheim, Germany, 2002. (c) Kantchev, E. A. B.; O'Brien, C. J.; Organ, M. G. *Angew. Chem., Int. Ed.* **2007**, *46*, 2768.
- (5) (a) Bourissou, D.; Guerret, O.; Gabbai, F. P.; Bertrand, G. *Chem. Rev.* **2000**, *100*, 39. (b) Crudden, C. M.; Allen, D. P. *Coord. Chem. Rev.* **2004**, *248*, 2247. (c) Hahn, F. E.; Jahnke, M. C. *Angew. Chem., Int. Ed.* **2008**, *47*, 3122. (d) Arduengo, A. J.; Bertrand, G. *Chem. Rev.* **2009**, *109*, 3209. (e) Nelson, D. J.; Nolan, S. P. *Chem. Soc. Rev.* **2013**, *42*, 6723. (f) Hopkinson, M. N.; Richter, C.; Schedler, M.; Glorius, F. *Nature* **2014**, *510*, 485. (g) Poyatos, M.; Mata, J. A.; Peris, E. *Chem. Rev.* **2009**, *109*, 3677.
- (6) For example, see: (a) Cesar, V.; Bellemin-Laponnaz, S.; Gade, L. H. *Chem. Soc. Rev.* **2004**, *33*, 619. (b) Marion, N.; Nolan, S. P. *Chem. Soc. Rev.* **2008**, *37*, 1776. (c) Poyatos, M.; Mata, J. A.; Peris, E. *Chem. Rev.* **2009**, *109*, 3677.
- (7) Herrmann, W. A. *Angew. Chem., Int. Ed.* **2002**, *41*, 1290.
- (8) Crabtree, R. H. *J. Organomet. Chem.* **2005**, *690*, 5451.
- (9) For selected examples of phosphine–NHC hybrid systems, see: (a) Lappert, M. F.; Maskell, R. K. *J. Organomet. Chem.* **1984**, *264*, 217. (b) Focken, T.; Raabe, G.; Bolm, C. *Tetrahedron: Asymmetry* **2004**, *15*, 1693. (c) Chiu, P. L.; Lee, H. M. *Organometallics* **2005**, *24*, 1692. (d) Song, G.; Zhang, Y.; Li, X. *Organometallics* **2008**, *27*, 1936. (e) Wolf, J.; Labande, A.; Daran, J.-C.; Poli, R. *Eur. J. Inorg. Chem.* **2008**, *2008*, 3024. (f) Naziruddin, A.; Hepp, A.; Pape, T.; Hahn, F. E. *Organometallics* **2011**, *30*, 5859. (g) Wheaton, C. A.; Bow, J.-P. J.; Stradiotto, M. *Organometallics* **2013**, *32*, 6148. (h) Gu, P.; Zhang, J.; Xu, Q.; Shi, M. *Dalton Trans.* **2013**, *42*, 13599. (i) Liu, X.; Braunstein, P. *Inorg. Chem.* **2013**, *52*, 7367. (j) Gradert, C.; Stucke, N.; Krahermer, J.; Näther, C.; Tuzek, F. *Chem. - Eur. J.* **2015**, *21*, 1130. (k) Atzrodt, J.; Dardau, V.; Kerr, W. J.; Reid, M.; Rojahn, P.; Weck, R. *Tetrahedron* **2015**, *71*, 1924.
- (10) Grubbs, R. H. *Angew. Chem., Int. Ed.* **2006**, *45*, 3760.
- (11) (a) Scholl, M.; Trnka, T. M.; Morgan, J. P.; Grubbs, R. H. *Tetrahedron Lett.* **1999**, *40*, 2247. (b) Huang, J.; Stevens, E. D.; Nolan,

S. P.; Petersen, J. L. *J. Am. Chem. Soc.* **1999**, *121*, 2674. (c) Scholl, M.; Ding, S.; Lee, C. W.; Grubbs, R. H. *Org. Lett.* **1999**, *1*, 953.

(12) Weskamp, T.; Schattenmann, W. C.; Spiegler, M.; Herrmann, W. A. *Angew. Chem., Int. Ed.* **1998**, *37*, 2490.

(13) Lummiss, J. A. M.; Beach, N. J.; Smith, J.; Fogg, D. E. *Catal. Sci. Technol.* **2012**, *2*, 1630.

(14) (a) Fantasia, S.; Egbert, J. D.; Jurčik, V.; Cazin, C. S. J.; Jacobsen, H.; Cavallo, L.; Heinekey, D. M.; Nolan, S. P. *Angew. Chem., Int. Ed.* **2009**, *48*, 5182. (b) Jurčik, V.; Nolan, S. P.; Cazin, C. S. J. *Chem. - Eur. J.* **2009**, *15*, 2509. (c) Jurcik, V.; Schmid, T. E.; Dumont, Q.; Slawin, A. M. Z.; Cazin, C. S. J. *Dalton Trans.* **2012**, *41*, 12619. (d) Broggi, J.; Jurčik, V.; Songis, O.; Poater, A.; Cavallo, L.; Slawin, A. M. Z.; Cazin, C. S. J. *J. Am. Chem. Soc.* **2013**, *135*, 4588. (e) Hartmann, C. E.; Jurcik, V.; Songis, O.; Cazin, C. S. J. *Chem. Commun.* **2013**, *49*, 1005. (f) Schmid, T. E.; Jones, D. C.; Songis, O.; Diebolt, O.; Furst, M. R. L.; Slawin, A. M. Z.; Cazin, C. S. J. *Dalton Trans.* **2013**, *42*, 7345. (g) Songis, O.; Cazin, C. S. J. *Synlett* **2013**, *24*, 1877.

(15) (a) Schuster, O.; Yang, L.; Raubenheimer, H. G.; Albrecht, M. *Chem. Rev.* **2009**, *109*, 3445. (b) Melaimi, M.; Soleilhavou, M.; Bertrand, G. *Angew. Chem., Int. Ed.* **2010**, *49*, 8810. (c) Donnelly, K. F.; Petronilho, A.; Albrecht, M. *Chem. Commun.* **2013**, *49*, 1145. (d) Crabtree, R. H. *Coord. Chem. Rev.* **2013**, *257*, 755. (e) Albrecht, M. *Adv. Organomet. Chem.* **2014**, *62*, 111.

(16) For selected examples, see: (a) Lebel, H.; Janes, M. K.; Charette, A. B.; Nolan, S. P. *J. Am. Chem. Soc.* **2004**, *126*, 5046. (b) Heckenroth, M.; Kluser, E.; Neels, A.; Albrecht, M. *Angew. Chem., Int. Ed.* **2007**, *46*, 6293. (c) Heckenroth, M.; Neels, A.; Garnier, M. G.; Aebi, P.; Ehlers, A. W.; Albrecht, M. *Chem. - Eur. J.* **2009**, *15*, 9375. (d) Ung, G.; Bertrand, G. *Chem. - Eur. J.* **2011**, *17*, 8269. (e) Krüger, A.; Albrecht, M. *Chem. - Eur. J.* **2012**, *18*, 652. (f) Khlebnikov, V.; Heckenroth, M.; Müller-Bunz, H.; Albrecht, M. *Dalton Trans.* **2013**, *42*, 4197.

(17) (a) Yang, L.; Krüger, A.; Neels, A.; Albrecht, M. *Organometallics* **2008**, *27*, 3161. (b) Kruger, A.; Neels, A.; Albrecht, M. *Chem. Commun.* **2010**, *46*, 315.

(18) The ^{31}P NMR resonance frequencies of **3b** do not agree with the literature data (see ref 17a). The newly determined chemical shift values are, for *trans*-**3b**: $^{31}\text{P}\{\text{H}\}$ NMR (CD_2Cl_2 , 162 MHz): δ 21.1 ($^1J_{\text{PRh}} = 76.3$ Hz); for *cis*-**3b**: $^{31}\text{P}\{\text{H}\}$ NMR (CD_2Cl_2 , 162 MHz): δ 48.3 ($^1J_{\text{PRh}} = 115.1$ Hz, $^2J_{\text{PP}} = 6.7$ Hz), 24.6 ($^1J_{\text{PRh}} = 82.6$ Hz).

(19) The ratio of phosphine oxide (8% of total phosphine) is similar to the quantity of the ratio of a single doublet, suggesting formation of a monodentate phosphine complex with one phosphine residue oxidized and unavailable for chelation, or the formation of free dppe oxide and a species with enantiotopic phosphine residues. In addition, another isomer with an AB doublet in the ^{31}P NMR spectrum was detected in some 15%, together with *trans*-**3a** (35%) and *cis*-**3a** (34%) as the major species.

(20) Krüger, A.; Häller, L. J. L.; Müller-Bunz, H.; Serada, O.; Neels, A.; Macgregor, S. A.; Albrecht, M. *Dalton Trans.* **2011**, *40*, 9911.

(21) After 3 weeks in CD_2Cl_2 , *trans*-**4** (33%), *cis*-**4** (28%) were the major species in solution. Moreover, dppe oxide (8%) was present and two C_s -symmetric and two C_1 -symmetric species in 17%, 7%, 6%, and 1%, with the following respective $^{31}\text{P}\{\text{H}\}$ NMR data (162 MHz): 17% species: δ 37.5 (dd, $^1J_{\text{PRh}} = 78.3$ Hz, $^2J_{\text{PP}} = 5.1$ Hz), 34.8 (dd, $^1J_{\text{PRh}} = 83.2$ Hz, $^2J_{\text{PP}} = 5.1$ Hz); 7% species δ 31.9 (d, $^1J_{\text{PRh}} = 84.4$ Hz). 6% species: δ 50.0 (dd, $^1J_{\text{PRh}} = 138.0$ Hz, $^2J_{\text{PP}} = 7.6$ Hz), 29.8 (dd, $^1J_{\text{PRh}} = 80.2$ Hz, $^2J_{\text{PP}} = 7.6$ Hz); 1% species: δ 57.4 (d, $^1J_{\text{PRh}} = 131.3$ Hz).

(22) Dissolving crystals in gave spectra that were in full agreement with *trans*-**4**. In addition, minor quantities of a solvento complex were detected due to the presence of cocrystallized H_2O .

(23) See, for example: (a) Poyatos, M.; Sanau, M.; Peris, E. *Inorg. Chem.* **2003**, *42*, 2572. (b) Mata, J. A.; Chianese, A. R.; Miecznikowski, J. R.; Poyatos, M.; Peris, E.; Faller, J. W.; Crabtree, R. H. *Organometallics* **2004**, *23*, 1253. (c) Leung, C. H.; Incarvito, C. D.; Crabtree, R. H. *Organometallics* **2006**, *25*, 6099. (d) Türkmen, H.; Pape, T.; Hahn, F. E.; Cetinkaya, B. *Eur. J. Inorg. Chem.* **2008**, *2008*, 5418.

(24) Krüger, A.; Michaud, G.; Dowling, A.; Müller-Bunz, H.; Albrecht, M. *Z. Anorg. Allg. Chem.* **2015**, *641*, 2250.

(25) Hartwig, J. *Organotransition Metal Chemistry*; University Science Books: Mill Valley, CA, 2010.

(26) (a) Guionneau, P.; Marchivie, M.; Bravic, G.; Létard, J. F.; Chasseau, D. *Top. Curr. Chem.* **2004**, *234*, 97. (b) Halcrow, M. A. *Coord. Chem. Rev.* **2009**, *253*, 2493.

(27) (a) Zassinovich, G.; Mestroni, G.; Gladiali, S. *Chem. Rev.* **1992**, *92*, 1051. (b) Klomp, D.; Hanefeld, U.; Peters, J. A. in *The Handbook of Homogeneous Hydrogenation*; de Vries, J. G., Elsevier, C. J., Eds.; Wiley-VCH: Weinheim, Germany, 2007; p 585. (c) Samec, J. S. M.; Bäckvall, J.-E.; Andersson, P. G.; Brandt, P. *Chem. Soc. Rev.* **2006**, *35*, 237. (d) Gladiali, S.; Alberico, E. *Chem. Soc. Rev.* **2006**, *35*, 226. (e) Clapham, S. E.; Hadzovic, A.; Morris, R. H. *Coord. Chem. Rev.* **2004**, *248*, 2201. (f) Wang, D.; Astruc, D. *Chem. Rev.* **2015**, *115*, 6621.

(28) Notably, this catalyst activity is still 1–2 orders of magnitude lower than that of the most active ruthenium and iridium systems known to date. See, for example: (a) Mestroni, G.; Zassinovich, G.; Camus, A.; Martinelli, F. J. *Organomet. Chem.* **1980**, *198*, 87. (b) Yang, H.; Alvarez, M.; Lugan, N.; Mathieu, R. J. *Chem. Soc., Chem. Commun.* **1995**, 1721. (c) Dani, P.; Karlen, T.; Gossage, R. A.; Gladiali, S.; van Koten, G. *Angew. Chem., Int. Ed.* **2000**, *39*, 743. (d) Albrecht, M.; Miecznikowski, J. R.; Samuel, A.; Faller, J. W.; Crabtree, R. H. *Organometallics* **2002**, *21*, 3596. (e) Thoumazet, C.; Melaimi, M.; Ricard, L.; Mathey, F.; Le Floch, P. *Organometallics* **2003**, *22*, 1580. (f) Baratta, W.; Chelucci, G.; Gladiali, S.; Siega, K.; Toniutti, M.; Zanette, M.; Zangrando, E.; Rigo, P. *Angew. Chem., Int. Ed.* **2005**, *44*, 6214. (g) For a spectacularly active system with iron, see: You, W.; Lough, A. J.; Li, Y. F.; Morris, R. H. *Science* **2013**, *342*, 1080.

(29) See the [Supporting Information](#) for more details.

(30) (a) Mashima, K.; Abe, T.; Tani, K. *Chem. Lett.* **1998**, 1199. (b) Murata, K.; Ikariya, T.; Noyori, R. *J. Org. Chem.* **1999**, *64*, 2186. (c) Polborn, K.; Severin, K. *Eur. J. Inorg. Chem.* **2000**, *2000*, 1687. (d) Matharu, D. S.; Morris, D. J.; Kamamoto, A. M.; Clarkson, G. J.; Wills, M. *Org. Lett.* **2005**, *7*, 5489. (e) Mao, J.; Baker, D. C. *Org. Lett.* **1999**, *1*, 841.

(31) For a base-free transfer hydrogenation system, see: (a) Corberan, R.; Peris, E. *Organometallics* **2008**, *27*, 1954. See also: (b) Zeng, F.; Yu, Z. *Organometallics* **2008**, *27*, 6025.

(32) Horn, S.; Gandolfi, C.; Albrecht, M. *Eur. J. Inorg. Chem.* **2011**, *2011*, 2863.

(33) (a) Noyori, R. *Angew. Chem., Int. Ed.* **2013**, *52*, 79. (a1) Noyori, R.; Ohkuma, T. *Angew. Chem., Int. Ed.* **2001**, *40*, 40. (b) Noyori, R.; Ohkuma, T.; Kitamura, M.; Takaya, H.; Sayo, N.; Kumobayashi, H.; Akuragawa, S. *J. Am. Chem. Soc.* **1987**, *109*, 5856. (c) Takaya, H.; Akutagawa, S.; Noyori, R. *Org. Synth.* **1989**, *67*, 20.

(34) The less shielded doublet of doublets at $\delta_{\text{P}} = 7.66$ is broad at room temperature and well resolved at -20 °C, which may point to dynamic coordination of the corresponding phosphine site.

(35) The more deshielded resonance at $\delta_{\text{P}} = 9.0$ shows a large $^1J_{\text{PRh}}$ coupling of 121.2 Hz, consistent with a *trans* MeCN ligand, while the more shielded signal at $\delta_{\text{P}} = 5.0$ ppm shows a smaller $^1J_{\text{PRh}}$ coupling constant of 78.7 Hz ($^2J_{\text{PP}} = 21.1$ Hz) indicating a *trans* carbene.

(36) Complex **8** (32 mg, 23 μmol) and AgBF_4 (18 mg, 94 μmol) were stirred for 16 h at room temperature in MeCN (5 mL). The suspension was filtered through Celite and eluted with MeCN (10 mL). Evaporation of the filtrate to dryness gave the solvent complex as a pale yellow solid (31 mg, quantitative). Crystals suitable for X-ray diffraction studies were obtained by slow diffusion of Et_2O into a MeCN solution of the complex. $^{31}\text{P}\{\text{H}\}$ NMR (CD_3CN , 162 MHz): δ 30.6 (dd, $^1J_{\text{PRh}} = 127.6$ Hz, $^2J_{\text{PP}} = 27.5$ Hz), 9.62 (dd, $^1J_{\text{PRh}} = 72.4$ Hz, $^2J_{\text{PP}} = 27.5$ Hz).

(37) Fujii, A.; Hashiguchi, S.; Uematsu, N.; Ikariya, T.; Noyori, R. *J. Am. Chem. Soc.* **1996**, *118*, 2521.

(38) Resonance frequency deduced indirectly by HSQC or HMBG experiments.

(39) This complex was not available in sufficient quantities after recrystallization for elemental analysis.

(40) Sheldrick, G. M. *Acta Crystallogr., Sect. A: Found. Crystallogr.* **2008**, *64*, 112.

(41) Spek, A. L. *J. Appl. Crystallogr.* **2003**, *36*, 7.